NUANCE, a giant protein connecting the nucleus and actin cytoskeleton

Yen-Yi Zhen, Thorsten Libotte, Martina Munck, Angelika A. Noegel and Elena Korenbaum

Institute for Biochemistry, Medical Faculty, University of Cologne, 50931 Cologne, Germany

Author for correspondence (e-mail: noegel@uni-koeln.de)

Accepted 1 May 2002

Journal of Cell Science 115, 3207-3222 (2002) *© The Company of Biologists Ltd*

Summary

NUANCE (NUcleus and ActiN Connecting Element) was identified as a novel protein with an α-actinin-like actin-binding domain. A human 21.8 kb cDNA of NUANCE spreads over 373 kb on chromosome 14q22.1-q22.3. The cDNA sequence predicts a 796 kDa protein with an N-terminal actin-binding domain, a central coiled-coil rod domain and a predicted C-terminal transmembrane domain. High levels of NUANCE mRNA were detected in the kidney, liver, stomach, placenta, spleen, lymphatic nodes and peripheral blood lymphocytes. At the subcellular level NUANCE is present predominantly at the outer nuclear membrane and in the nucleoplasm. Domain analysis shows that the actin-binding domain binds to F-actin in vitro and colocalizes with the actin cytoskeleton in vivo as a GFP-fusion protein. The C-terminal transmembrane domain is responsible for the targeting the nuclear envelope. Thus, NUANCE is the first α-actinin-related protein that has the potential to link the microfilament system with the nucleus.

Key words: CH domain, Spectrin repeats, Klarsicht-like domain, Nuclear envelope

Introduction

Many biological processes depend on the balance between the dynamics and the stability of the actin cytoskeleton. The cellular organization of the microfilament system is therefore characterized by a large variability and flexibility. Proteins of the α-actinin superfamily utilize a double calponin homology domain to arrange actin filaments in bundles or meshworks and to link them to the plasma membrane (Matsudaira, 1994). The modular organization of the proteins of the α-actinin superfamily (Puius et al., 1998) allows the building of extremely long protein chains. The largest proteins mainly represent two families: plakins (plectin and dystonin) (Brown et al., 1995; Wiche, 1998) and spectrins (dystrophin, utrophin and spectrin itself) (Ahn and Kunkel, 1993; Tinsley et al., 1992). Plakins are characterized by a tripartite structure, where a central coiled-coil rod separates two globular domains: the N-terminal plakin domain and the C-terminal domain, which is composed of plectin repeats (Ruhrberg and Watt, 1997). The characteristic feature of spectrins is the rod domain, which is composed of multiple triple helical spectrin repeats (Pascual et al., 1997).

The identification of the *Drosophila* protein kakapo (also known as groovin) (Gregory and Brown, 1998; Prokop et al., 1998; Strumpf and Volk, 1998) and its mammalian homologue MACF (also described under the names trabeculin-α and macrophin) (Leung et al., 1999; Okuda et al., 1999; Sun et al., 1999), as well as BPAG1-a and BPAG1-b forms of the *BPAG/dystonin* locus (Leung et al., 2001b), brought confusion to this classification, since these proteins, which are larger than the other known plakin and spectrin proteins, harbor both domains found in plakin and spectrin and may represent a fusion product of two precursor genes. An alternative hypothesis proposes that the ancestral gene resembled the *shortstop/kakapo* genes of *Drosophila* and *Caenorhabditis* (Leung et al., 2001a). Owing to their multiple binding sites for microtubules, intermediate filaments and microfilaments, these giant proteins are recognized as cytolinkers, integrating the cytoplasmic cytoskeleton with membranes and submembrane complexes (Fuchs and Yang, 1999; Karakesisoglou et al., 2000).

The recently described protein calmin, which also possesses a N-terminal actin-binding domain (ABD) of the α-actinin type, does not fall into any of the above categories, as it does not harbor either a coiled-coil rod domain or any other common motifs (Ishisaki et al., 2001). Instead it has a C-terminal transmembrane domain (TMD) that targets cytoplasmic reticular structures and therefore represents the first integral membrane α-actinin-related protein known so far. However, some transcripts of calmin are differentially spliced and lack the TMD. The distribution pattern of the calmin isoforms did not overlap with that of the actin cytoskeleton. Here we report the molecular characterization and cellular localization of NUANCE, the largest known protein of the α-actinin superfamily. The 796 kDa protein harbors multiple dystrophin-like spectrin repeats but lacks domains characteristic for plakins. Hence, it is related to the spectrin family of the α-actinin superfamily. Unlike other related proteins, NUANCE is associated with the nuclear envelope (NE) via the predicted TMD. This enormously large protein may harbor numerous binding sites and serve as a scaffold for the assembly of various protein complexes.

Materials and Methods

Molecular cloning

The clones AA480953 and AA761297, containing partial NUANCE

cDNA, were obtained from RZPD (Resource Center/Primary Database of German Human Genome Project) and fully sequenced. The full-length cDNA of NUANCE was cloned by using SMART RACE cDNA amplification kit (Clontech) and Advantage 2 polymerase (Clontech) with mRNA from Burkitt's lymphoma cells BL-60 as a template. With 5′-RACE-PCR we extended the cDNA to the putative 5′ end (fragment 1, Fig. 1A). Several rounds of 3′-RACE-PCR extended the cDNA to a total length of 6.1 kb (fragments from 2 to 5, Fig. 1A). Close inspection of the publicly accessible genomic sequence (GenBank) downstream of the identified NUANCE partial cDNA revealed a polyadenylated cDNA of DKFZp434G173 (accession number AL080133), which encoded several spectrin repeats, similar to those found in NUANCE. This suggested that the amplified 6.1 kb fragment of NUANCE and DKFZp434G173 cDNAs represent the 5′ and 3′ end of the same giant transcript. The ESTs matching the genomic DNA from the gap region, which encoded peptides with homology to dystrophin-like spectrin repeats, were used to design supplementary primers. The PCR products were cloned into the pGEM T-Easy vector (Promega) and sequenced. 22 clones containing partial NUANCE cDNAs were used to assemble full-length NUANCE cDNA (accession number AF435011). The cDNA of the short ABD-S isoform has been deposited under accession number AF435010. Partial mouse NUANCE cDNAs from RT-PCR of kidney RNA with the primers designed from the sequence of EST clones AI747790 and AA498987 were deposited under accession number AF435012.

Expression analyses

The expression profile of human NUANCE was studied by probing a human multiple tissue expression array (Clontech). The cDNA probe encompassing nucleotides from 247 to 1443, which corresponds to the NUANCE ABD with the following spectrin repeat, was ^{32}P-labeled using a random prime labeling kit (Stratagene). As a control, the blot was stripped and reprobed with ubiquitin.

Production of the recombinant proteins in *E. coli* and generation of the monoclonal antibodies

DNA fragments encoding the first 285 (6×His-ABD) and 459 amino acid residues (6×His-ABD-l) were obtained by PCR using fragment 2 as a template and inserted into pQE-30 (Qiagen). Recombinant proteins were induced by IPTG in *E. coli* M15[pREP4] and purified using a Ni-NTA agarose column according to the manufacturer (Qiagen). mAb K20-478 was produced by immunizing mice with the purified 6×His-ABD-l protein with ImmunEasy mouse adjuvant (Qiagen) as described earlier (Olski et al., 2001).

Actin-binding assay

The F-actin co-sedimentation assay and the quantification of 6×His-ABD bound to F-actin was performed as described previously (Olski et al., 2001). For high- and low-speed centrifugation assays, samples were pelleted at 125,000 ***g*** and at 20,000 ***g***, respectively. Actin polymerization was measured by recording the changes in fluorescence intensity of pyrene-labeled α-actin monomers as described previously (Korenbaum et al., 1998). The fluorescence measurements were made using a Fluoroskan Ascent FL plate reader (Labsystems). Polymerization of 8 μM actin alone or in the presence of various amounts of the ABD was initiated by addition of 2 mM $MgCl_2$ and 100 mM KCl.

Plasmid construction and transient transfections

The constructs GFP-ABD (residues 1-296) and GFP-ABD-S (residues 1-262 with additional amino acids AYKN from exon 8a) were amplified from fragment 2 and 2a, which code for spliced variants, using primers with extensions for *Bam*HI and *Kpn*I sites and cloned into *Bgl*II/*Kpn*I-cut pEGFP-C1 (Clontech). For the GFP-ABDsr1-2 construct (residues 1-531), fragment 2 was digested with *Bam*HI and *Eco*RI then ligated into *Bgl*II/*Eco*RI-cut pEGFP-C1 vector. For the GFP-sr15-21 (residues 5727-6596), the fragment 13a was excised utilizing the *Eco*RI sites of pGEM T-Easy (Promega) and ligated into *Eco*RI site of pEGFP-C1. For the GFP-Cterm1 construct (residues 6571-6885), the cDNA was amplified from clone 13 and ligated into *Eco*RI-cut pEGFP-C2 vector. For the GFP-Cterm2 constructs, clone 13b was digested with *Sac*I and *Eco*RI and inserted into corresponding sites of pEGFP-C1. The GFP-Cterm2Δtm (residues 6642-6834 with additional 14 amino acids from the extended exon 111) lacking the putative TMD was generated from the GFP-Cterm2 by *Pst*I digestion and religation. To generate GFP-NUA$^{\Delta 460\text{-}6643}$, the GFP-ABDsr1-2 was cut with *Kpn*I and *Bam*HI and ligated with the insert of the GFP-Cterm1 (residues 6643-6885), which was amplified using the primers with added-on *Kpn*I and *Bgl*II sites. COS7 cells were transfected by electroporation. The expression of the fusion proteins was controlled by western blotting using a GFP-specific mAb.

Cell culture

COS7 cells were grown in DME medium supplemented with 10% FBS (Sigma), 2 mM glutamine, penicillin and streptomycin. For the propagation of human embryonic kidney cells (293) pyruvate was added to the medium. Human T lymphocytes (Jurkat), Burkitt's lymphoma cells BL-60 and B-JAB were maintained in RPMI 1640 containing 10% FBS, 2 mM L-glutamine, penicillin and streptomycin. For Latrunculin A (Biomol) treatment, 70%-confluent COS-7 cells were fixed 15, 30 and 60 minutes after exposure to 1 μM LatA. The recovery was evaluated by culturing the cells in LatA-free medium for another 30, 60 and 90 minutes. For microtubule depolymerization the cells were incubated in medium containing 1 μM vincristine (Sigma) or 5 μg/ml colchicine (Fluka) for 4 hours before processing for immunofluorescence. To promote the formation of lamellipodia, confluent serum-starved monolayers of COS7 cells were wounded by scraping away cells with a P1000 pipet tip. The coverslips were then incubated in complete media for 6 hours prior to fixation.

Immunofluorescence

Adherent cells were allowed to attach onto glass coverslips for 1-16 hours, rinsed with PBS, fixed in 3% paraformaldehyde and permeabilized with 0.5% Triton X-100 in PBS for 5 minutes. Alternatively, cells were fixed with methanol at –20°C for 10 minutes. Generally, no difference was observed between the two fixation protocols except for the cells transfected with the GFP-Cterm2 construct. All figures display cells fixed with paraformaldehyde unless stated otherwise. For permeabilizing with digitonin, fixed cells (3%-paraformaldehyde) were washed in ice-cold PBS and treated with 40 μg/ml digitonin (Sigma) in PBS for 5 minutes on ice. For poorly adherent cells, cover slips were pretreated with poly-L-lysine (1 mg/ml), and cells were allowed to attach for at least 3 hours. Cells were incubated with mAbs against vinculin (Sigma), annexin A7 (Selbert et al., 1995), with the maD mAb, which is specific for β-COP (Pepperkok et al., 1993), with JOL2, which is specific for lamin A/C, with LN43, which is specific for anti-lamin B2 (kind gift from Frans Ramaekers and Jos Broers) or with polyclonal antibodies against Nup358 (kind gift from Elias Coutavas and Günter Blobel) and against NO38/B23 (kind gift from M. Schmidt-Zachmann). Cells washed with PBS were incubated with the appropriate secondary antibodies conjugated to Cy3 (Sigma), Alexa488 or Alexa568 (Molecular Probes) and mounted in Gelvatol/DABCO (Sigma). F-actin was detected with TRITC-labeled phalloidin; for nuclear staining the DNA-specific dye DAPI (Sigma) was used. Samples were analyzed by wide-field fluorescence microscopy (DMR, Leica) or confocal laser scanning microscopy (TCS-SP, Leica).

Cell fractionation and immunoblots

COS7 cells were harvested and washed in PBS, homogenized in lysis buffer (1% SDS, 1 mM sodium vanadate and 100 mM Tris-HCl, pH 7.4), incubated at 95°C for 5 minutes and mixed with the protein sample buffer (Laemmli, 1970) and heated again for 5 minutes to 95°C. Proteins were separated on 3-15% gradient SDS-PAGE then transferred onto PDVF membrane (Millipore). The membranes were treated with mAb K20-478 followed by enhanced chemiluminescence.

For nuclei preparation, COS7 cells were sonicated in hypotonic buffer (10 mM HEPES, pH 7.5, 1.5 mM $MgCl_2$, 1.5 mM KCl, 0.5 mM DTT, 0.2 mM PMSF) supplemented with Protease Inhibitor Cocktail CompleteTM, Mini (Boehringer Mannheim). Nuclei were sedimented at 1,000 ***g*** at 4°C for 15 minutes. For further fractionation the supernatant was centrifuged at 100,000 ***g*** for 30 minutes at 4°C. Both pellets were resuspended in hypotonic buffer and analyzed on immunoblots with anti-NUANCE, anti-lamin B2 (LN43) and anti-annexin A7 mAbs.

Computer programs

For alignment of cDNA sequences and database mining, the GCG software package and the BLAST (NCBI) program were used. Protein sequences were aligned using the programs ClustalW and TreeView. Motif predictions and pattern searches were performed with the ExPaSY (SIB) software package.

Results

Cloning and analysis of NUANCE cDNA

We searched for new proteins with homology to the ABD of α-actinin by screening the human EST database using the peptide sequence of ABDs of known α-actinin-related proteins as a query. Two overlapping ESTs, AA480953 and AA761297, were identified that contained a partial cDNA encoding for a novel protein with an ABD that was highly homologous to MACF (Leung et al., 1999) and plectin (Wiche et al., 1991). Both clones were derived from a cDNA library prepared from human tonsillar cells enriched for germinal center B cells. Combining RACE-PCR with the analysis of data available from human non-redundant EST and human genomic GenBank databases, we cloned 21.8 kb of NUANCE cDNA (see Materials and Methods; Fig. 1A). The putative ATG start codon at position 205 together with the surrounding sequence AGAATGG matched the Kozak consensus (Kozak, 1987). An in-frame stop codon was located 26 bp upstream, making this ATG the translational start site. The 3′ untranslated region (3′UTR) of 910 bases ends in a poly(A) tail. A polyadenylation signal, ATTAAA, is located 22 nucleotides upstream of the poly(A) addition site.

Genomic DNA organization

To analyse the intron-exon organization of NUANCE and to identify the alternatively spliced isoforms, we searched the genomic database and found that the *NUANCE* gene matched the publicly available working draft sequences of human clones with the accession numbers AL355100.2, AL162832.3, AL359235.2, AL355094.2, AF215937.1, AL352983.2 and AL161756.3 of chromosome 14 in contig NT_025892 mapped to 14q22.1-q22.3 (Fig. 1B). The human *NUANCE* gene spans over 373 kb. About 6 kb downstream the *NUANCE* gene is the estrogen receptor 2 gene (*ESR2*).

The *NUANCE* gene is split into 115 recognizable exons (Fig. 1B, Table 1). All exon-intron boundaries are consistent with the consensus sequence for splice junctions 5′-GT…AG-3′ (Breathnach and Chambon, 1981). The intronic sequences comprise 94% of the total gene length. The 5′UTR is interrupted by the longest 55,954 bp intron located 42 bp upstream of the start codon, therefore translation starts in the second exon. An alternatively spliced form with the exon 1a positioned 228 bp upstream of exon 1 was found in the EST BI026470. The exon lengths vary from 50 nt in exon 114 to 2101 nt in the exon 48 coding for central coiled-coil sequences.

Exons 3 to 9 encode the ABD region of NUANCE. One of the ABD fragments amplified by RACE-PCR (clone 2a) contained an additional exon 8a (Fig. 1C) inserted between exons 8 and 9. This leads to premature termination of the ORF and generation of an isoform comprising a truncated ABD, named ABD-S. Although the physiological relevance of ABD-S is not yet clear, the effect of ABD-S overexpression was analyzed in transfection experiments (see below; Fig. 9B,E). Several differentially spliced cDNAs corresponding to the 3′end of the NUANCE cDNA were found in the non-redundant NCBI database. The cDNAs with accession numbers AK001876, AL080133, AB023228, which correspond to a protein KIAA1011 (Syne-2), may represent a partial sequence of *NUANCE*, since their ORF is not interrupted by any Stop codons upstream of the methionine proposed as a translation initiation in AL080133. The cDNA with accession number AL117404 appears to contain a short isoform with a distinct 5′ terminus (Fig. 1D). However, it can also result from amplification of unprocessed mRNA.

Structural features of NUANCE

The NUANCE ORF encodes a protein of 6,885 amino acids with a molecular mass of 796,000 (Fig. 2). The theoretical pI is 5.29. Three distinct structural domains can be distinguished: the N-terminal ABD (Fig. 3A,B), which is followed by a long largely helical rod domain (Fig. 3A,E) and a C-terminal TMD (Fig. 3A,D).

The ABD of NUANCE shares a high homology with the ABDs of the recently identified proteins enaptin (S. Braune, MD Thesis, University of Cologne, 2001) and calmin (Ishisaki et al., 2001). The ABDs of these three proteins differ from the conventional ones as they have 30 amino-acids long linkers between two CH domains (Fig. 3B). Across its 255 amino acid ABD region, NUANCE shares about 49% identity with enaptin, 45% with calmin and 43% with β-spectrin, plectin, dystonin and MACF. The phylogenetic analysis of the ABDs suggested that NUANCE, enaptin and calmin form a distinct family within the α-actinin superfamily (Fig. 3C). BLAST searches with human NUANCE cDNA identified several highly homologous mouse EST clones. On the basis of the sequence of EST clones AI747790 and AA498987, we have designed primers and amplified a partial mouse NUANCE cDNA. The amino-acid sequence of the mouse and human NUANCE ABD is well conserved with an identity of 97%.

A central rod domain contains coiled coils interrupted by several fragments of random coils. Furthermore, four nuclear localization signals (amino acids 1188-1205, 1464-1467, 3629-3645 and 6115-6132) and two leucine zippers (amino acids 2127-2148 and 5008-5029) were also predicted by computer

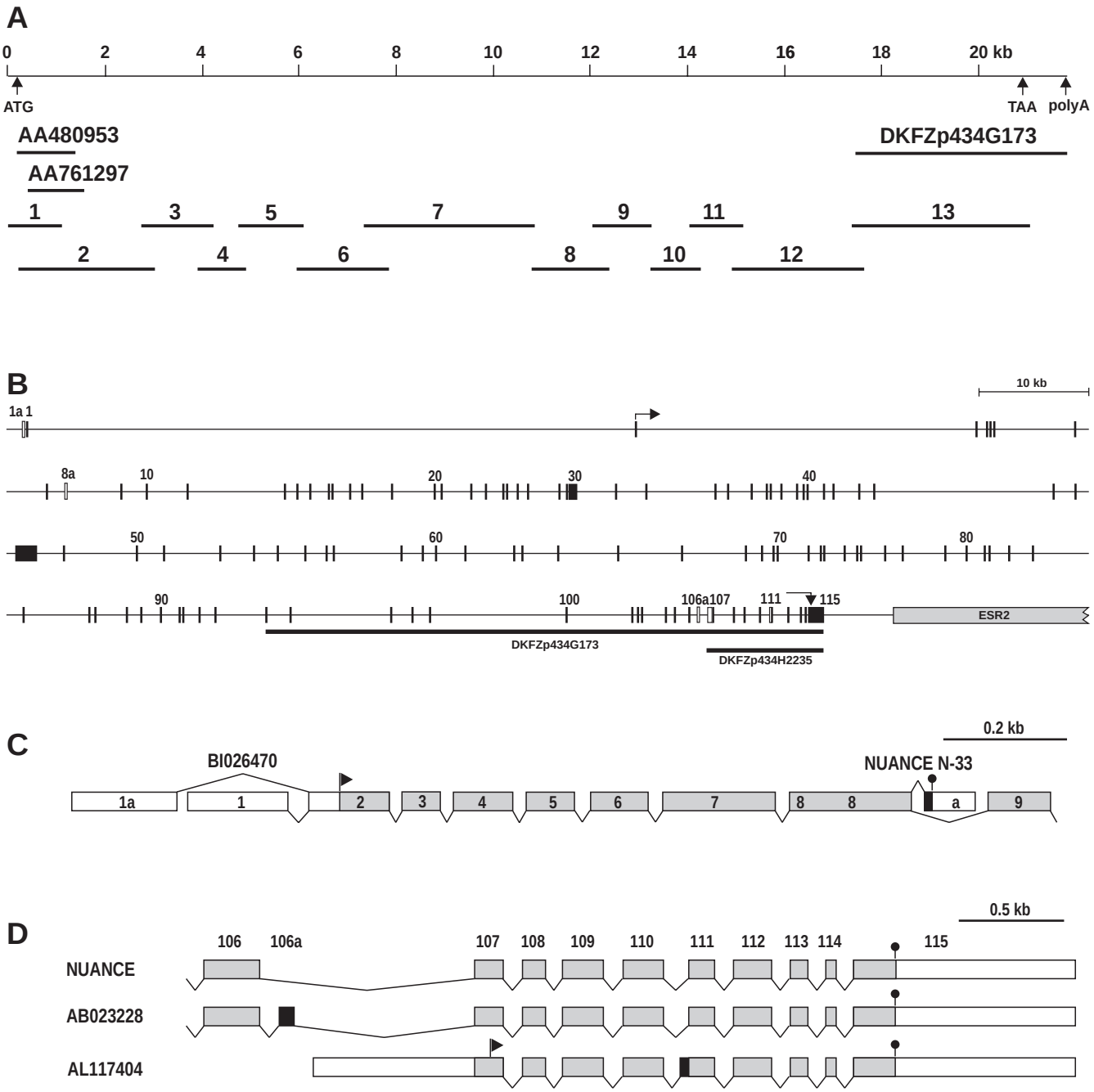

Fig. 1. Cloning of the human *NUANCE* gene. (A) The 21.8 kb cDNA was assembled from 13 overlapping clones obtained by RT- and RACE-PCR using mRNA from BL-60 cells as the template. (B) The exon-intron organization of the human *NUANCE* gene. The *NUACE* gene contains 114 protein-coding exons. Introns, represented by lines, are drawn to scale; exons are shown as vertical bars. Exon 1a, found in the EST BI026470, exon 8a, found in the short isoform NUANCE-ABD-S, exon 103a, found in the KIAA1011 protein (accession number AB023228), and the longer form of exon 104, which is found in DKFZp434H2235 mRNA (accession number AL117404), are represented by empty bars. The positions of Start and Stop codons are indicated by arrows. The annotated sequences of DKFZp434G173 (accession number NM_015180) and DKFZp434H2235 are underlined by solid lines. The estrogen receptor 2 gene (*ESR2*) located downstream is boxed. Alternative splicing at the 5′ end (C) and at the 3′ end (D) of the *NUANCE* gene. An additional exon 1a that encodes an alternative transcriptional start was found in EST BI026470. The boxes represent exons drawn to scale. Gray shading indicate coding regions; white boxes indicate untranslated regions. Aternatively spliced coding exons are shown in black. The locations of the ATG start codon and the TGA stop codon are indicated. The size of each exon and intron is given in Table 1.

analysis within the rod domain (Fig. 3A). Multiple repeated units weakly homologous to the triple-helical spectrin-like repeats of dystrophin and utrophin can be recognized in the regions predicted for two- and three-stranded coiled coils (Fig. 3E). The repeats found in NUANCE are less regular than the ones of dystrophin and utrophin (Winder et al., 1995). The

Table 1. Exon-intron organization of the human *NUANCE* gene

Exon no.	Sequence at exon-intron boundary		Exon size (bp)	Intron size (bp)	Exon no.	Sequence at exon-intron boundary		Exon size (bp)	Intron size (bp)
	5′ splice donor	5′ splice acceptor				5′ splice donor	5′ splice acceptor		
1a	AGCCCG	CCCCGG/gtaaga	170	228	59	ttctag/GATGTG	GGGGAG/gtaagc	121	1,168
1	GCCAAG	CGGACG/gtgggt	161	55,963	60	attaag/GTCATA	TTAAAG/gtaagc	183	2,300
2	tttcag/TTCACT	TGCAAG/gtaatt	130	31,386	61	ttatag/GTAGTC	CTACAG/gtatgt	132	4,463
3	tgatag/CTGAAC	GCCAGG/gtaagc	62	1,018	62	acacag/GGAGAA	CGGAAG/gtgggt	198	600
4	ctgcag/CACACT	CAGTTG/gtaaga	96	94	63	tttcag/TTGAAC	AGCGAT/gtaagg	75	3,110
5	tcacag/CCTCGG	CGATCA/gtaagt	78	88	64	tgatag/AATGGA	TGTTCA/gtaatg	123	5,435
6	ttccag/ATTAAG	TTTCAT/gtaagt	93	7,686	65	ttacag/GAAGCA	GAAGAG/gtaagt	117	5,743
7	ccttag/ATTGAG	CGCCAC/gtaagt	182	4,718	66	tcttag/GGCACC	TGCCAG/gtaaga	231	5,855
8	tgatag/CTATGA	CAGAAG/gtaaag	197	1,514	67	tcctag/GCTATG	GATCAG/gtaaaa	183	1,317
8a	aaccag/CTTACA	GACCAG/gtgact	82	5,012	68	ttgcag/CATCCT	CAACAG/gtaatt	135	959
9	ttgcag/ATGTGG	GCTCAG/gtatgt	101	2,273	69	ttacag/GTTCTG	TGCAAG/gtaaaa	122	152
10	atacag/GGAAAG	TATAAT/gtaagt	102	3,708	70	caaaag/CAACCA	CCTCAG/gtcagt	142	2,651
11	ttgcag/AGCCTG	CACCAG/gtgact	138	8,616	71	aaatag/GTTTCC	ACACAG/gtagaa	132	1,066
12	tttcag/ATTAAT	TTCAAG/gttgga	165	1,117	72	attcag/GAAAAT	TACGAG/gtaggg	153	118
13	tttcag/AGCCTG	AAGACG/gtgtgt	113	834	73	ctccag/ACGCTG	TACCAG/gtatga	210	1,644
14	ttccag/AATCAA	TGGCAT/gtaagc	163	1,639	74	ttacag/AATGAA	CTTCAG/gtaatc	102	1,228
15	tcccag/AAATTT	ATTTGG/gtaaag	79	247	75	acttag/AAAGCA	TTAGAG/gtatgc	120	146
16	ttgtag/CTGGAG	AAAGAG/gtattt	189	1,457	76	tttcag/GATGTA	CACAAG/gtgaga	201	2,016
17	atgtag/GTACCC	CAACTT/gtaagt	165	942	77	tcatag/GTTTTT	TTGCAG/gtattt	174	1,630
18	gtatag/GAAATG	ATAAAG/gtaaaa	150	2,569	78	ctctag/AAATGG	TACCAG/gtattt	132	3,586
19	ttgtag/GCTGGA	TTGAAG/gtatgt	162	4,793	79	tattag/CAAATA	GCTCAG/gtcagc	197	2,037
20	taatag/CATCTT	GTCCAG/gtctct	159	372	80	tgttag/TTATAA	TTTTTT/gtaagt	133	1,367
21	ttcaag/ATCAAT	CACAAG/gtggga	174	2,718	81	ctttag/GAGTTT	CACCAG/gtaagt	183	418
22	ttttag/GAAGCA	TGGGAG/gtaaga	135	1,074	82	ttacag/CTTCAA	CACAAG/gtaatt	147	1,683
23	ttgtag/TCTCTT	CATGAG/gtacaa	159	1,744	83	ttttag/GAGTTT	AGAAAG/gtgtgt	177	2,119
24	aattag/GCCTGC	AAACGA/gttagt	212	142	84	acttag/ATACAA	TGTCAG/gtgagg	156	6,639
25	ttctag/GGGGAC	GAAAAG/gtgtta	91	827	85	ttccag/GATATA	ACTCAG/gtacta	153	5,908
26	ccttag/GCAATG	AGAGAG/gtaaac	110	585	86	gtctag/GTCAAT	CTTCAG/gtaaat	171	456
27	gcccag/GTATGA	CTACAG/gtaatt	127	1,520	87	tcttag/TCTCTG	TAAAAG/gtatgc	131	2,629
28	atctag/GTCATA	TACCAG/gtaaaa	158	1,114	88	tgacag/GTGGAC	ATAAAG/gtgggt	205	1,125
29	acccag/AATGGA	CTAAGG/gtaagt	148	626	89	ctgcag/GAGCTG	TTTGAG/gttcat	180	1,703
30	ttttag/AATATC	ACATCG/gtaagt	611	3,704	90	ttctag/TTTGTT	TTCCTG/gtattg	126	1,822
31	atcaag/GAAAAA	CGAATG/gtaagg	180	2,743	91	aaatag/AATCAT	CTGCAG/gttaga	155	107
32	tcttag/TCTTGA	GCAGAG/gtgagt	151	6,356	92	ttgtag/TGAGCT	TATAAG/gtaaac	145	1,237
33	ttacag/ATTGAA	CTTGAT/gtaagt	159	963	93	atacag/ATGTTA	GAACAG/gtgagc	95	1,256
34	tggtag/ATAAAT	CTGAAG/gtaatt	162	2,235	94	ccccag/ACCAGA	CTGAAG/gtagtg	235	5,491
35	ttttag/GAAGAA	TTGCAG/gtaaga	102	1,221	95	tcttag/AATAAA	GTAGAG/gtaaac	195	2,219
36	tttcag/GTCATG	CTAGAG/gtgcta	201	341	96	aaatag/ACCTGG	ATTAAG/gtattg	126	8,940
37	atttag/GAGATA	TGAATG/gtgagt	172	722	97	atgcag/GAACTA	TTAAGG/gtaagt	156	1,970
38	ctgcag/ATCAAT	CTTTCT/gtaaga	113	1,383	98	ttgcag/GTGGCC	CAGAAG/gtaagg	159	1,422
39	ctgaag/GATTTC	ACTGAG/gtagga	203	452	99	tgccag/GACTGC	ATCAAG/gtaaga	167	13,563
40	ttttag/ACTCCA	AAAGAG/gtatag	120	98	100	gtgtag/GGTGAA	CAGCAG/gtggga	163	5,794
41	ttacag/GGAACA	ATCAAG/gtataa	292	1,157	101	tcacag/GATCTA	CATGAA/gtaaga	188	482
42	attcag/GAAATC	CCTAAG/gtaaag	152	753	102	catcag/AATCGA	TTTGAG/gtaaac	151	363
43	atttag/CCATCA	CTGCAG/gtgagg	310	2,101	103	atgcag/GCCTTT	CTCAGG/gtgagc	183	1,86
44	ttttag/GATTCT	CTGCAG/gtacta	165	976	104	ttgcag/CATTTC	CTGAAT/gtgagg	138	712
45	ttgtag/GAACTA	AACAAG/gtaagt	342	16,797	105	caacag/GGCTTC	ACTCCG/gtacgg	195	1,188
46	tttcag/GATTCA	ATAGAG/gtatgg	156	1,455	106	gtttag/GGCTTG	TGTCAG/gtaaca	277	1,777
47	ttttag/AAATTA	TAAAGT/gtaagt	266	1,682	106a	tttcag/ATGTAG	GAAAGC/gtcttc	61	
48	ttctag/AGGACC	CGCACA/gtaagt	2,101	2,286	107	tttcag/GTAAAT	CCCTAT/gtaagt	140	2,010
49	cactag/AATGTC	AGAAAG/gtaatc	323	2,287	108	ttctag/GGAAAG	AGTCAG/gtactg	115	695
50	cactag/GTATCT	CCAAAG/gtaata	145	5,466	109	ttccag/GTGCCT	CTGCAG/gtgagt	203	1,026
51	cttaag/GCCTTG	GAAGAA/gtgagt	219	4,994	110	tggtag/GAGATA	TGCCAG/gtacgc	201	938
52	aattag/ATTGAA	CAACAA/gtaaga	266	3,058	111	tttaag/GACTTC	CTAATG/gtaagt	129	1,484
53	ttttag/GCTTCT	TTTGAG/gtaagt	169	1,658	111a	ttccag/GGCTCT	CTAATG/gtaagt	171	1,484
54	ttttag/GAGCTT	GAGAAG/gtaata	156	2,505	112	tttcag/CAACTG	ACCCAG/gtgagt	192	1,080
55	tcacag/ATTAGC	CAAAAG/gtaaaa	141	1,849	113	tttcag/AACCCA	GCAAAG/gtaaga	84	448
56	gaacag/AAAATG	AATAAG/gtatgg	183	754	114	acccag/CAGTTC	GAGCAG/gtaacg	50	273
57	tcccag/GCCACA	GTGCAG/gtaagt	137	6,096	115	tggcag/GGTCCC	GCTTCT	1,114	
58	atctag/ATGGCT	GCTGAT/gtaagt	186	1,717					

alignment of the 22 best-defined NUANCE repeats are shown in Fig. 3E. The helix A is characterized by a highly conserved tryptophan followed by a hydrophobic residue. The first helix (helix A) and the last one (helix C), which are continuous in the following repeats, are relatively well defined, whereas the middle helix B is less ordered. Random coils in the regions 4082-4232, 4332-4532 and 6347-6547 (Fig. 3A) may represent hinges providing additional flexibility to the molecule.

In addition, the C-terminal region of NUANCE contains a 62 amino-acid region similar to the Syne-1 and *Drosophila* Klarsicht proteins, which are involved in nuclear migration and nuclear positioning (Apel et al., 2000; Mosley-Bishop et al.,

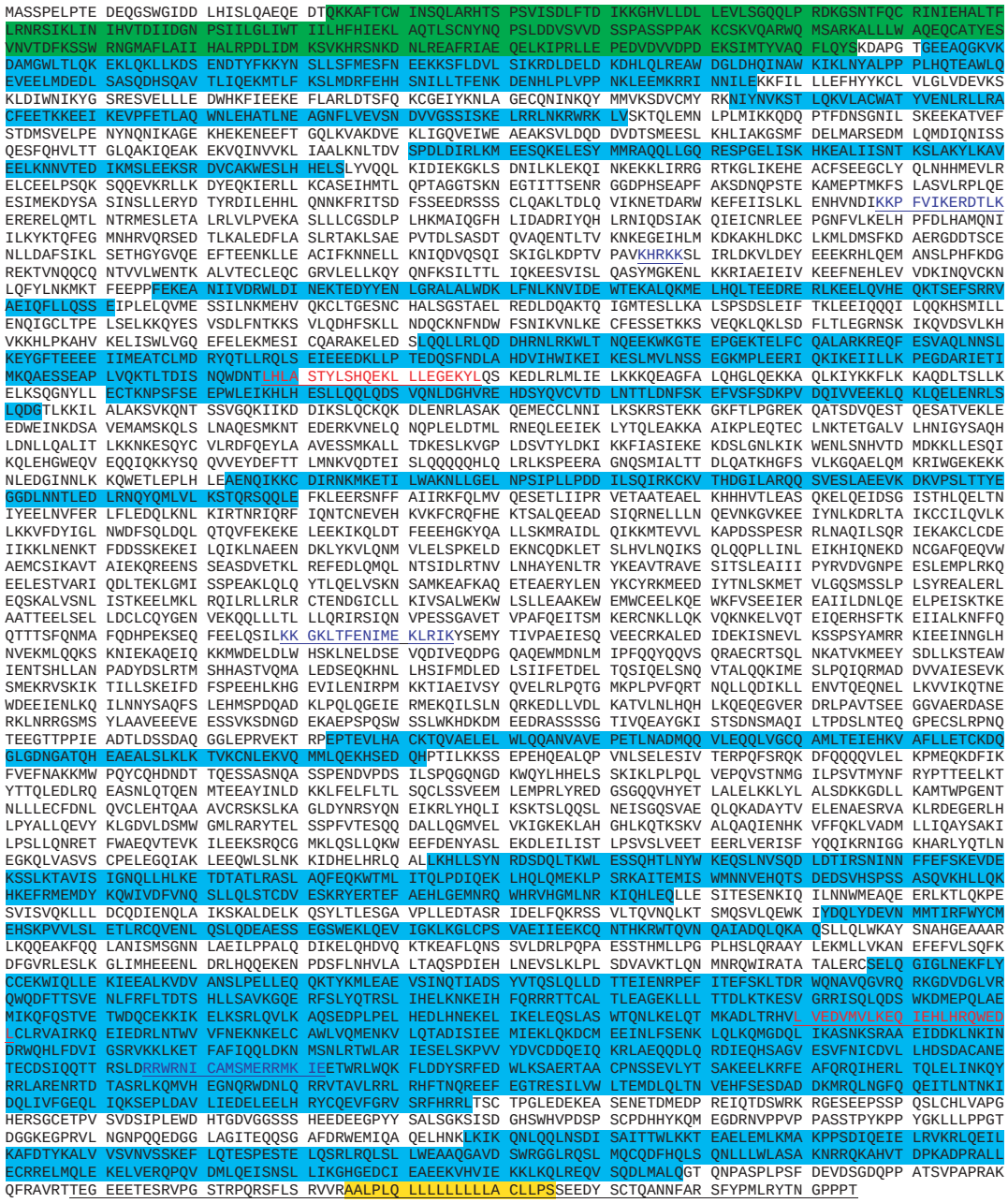

Fig. 2. Deduced polypeptide sequence of human NUANCE. Amino acid residues are numbered on the left. The actin binding domain of NUANCE is highlighted in green; 22 detected dystrophin-like spectrin repeats are in cyan, the transmembrane region is in yellow, Klarsicht-like domain is in black and underlined. Predicted nuclear localization signals are shown in blue and are underlined, leucine zippers are in red and underlined.

Fig. 3. Structural features of human NUANCE. (A) The ABD is represented by an empty box; 22 spectrin repeats with considerable homology to dystrophin are shown as filled ovals; and the TMD is indicated by a black bar. The positions of nuclear localization signals and leucine zippers are indicated. Coiled-coil regions were detected by the MultiCoil program (Wolf et al., 1997) with a window size of 21. Blue and red lines mark the location of predicted dimeric or trimeric coiled coils, respectively. (B) Alignment of the ABDs of NUANCE, enaptin, calmin (BAB59010), β-spectrin (AAA60580) and MACF (AAD32244). NUANCE, enaptin and calmin harbor long stretches between both CH domains unlike conventional ABDs of β-spectrin and MACF. (C) A phylogenetic tree of the ABDs of NUANCE and other proteins of the α-actinin superfamily on the basis of calculations from ClustalW alignment of these domains. The accession numbers are: human filamin (AF184126), human dystrophin (P11532), *Dictyostelium* cortexillin (L49527), human β-spectrin (M96803), *Drosophila* kakapo (AJ011924), *Dictyostelium* interaptin (AF057019), chicken fimbrin (A37097), mouse α-actinin (P12814), human utrophin (P46939), mouse plectin (AF188012), mouse MACF (AF150755), mouse dystonin (AF252549) and human calmin (BAB59010). (D) Klarsicht-like domain of NUANCE. The C-termini of NUANCE, human Syne-1 (KIAA0796 protein, BAA34516), mouse Syne-1 (AAG24392), human lymphocyte membrane associated protein (LMAP, AAC02992), an uncharacterised *C. elegans* protein similar to myosin-like proteins (AAF40010) and *D. melanogaster* Klarsicht protein (AAD43129) are aligned with ClustalW version 4.2. The amino acids similar in more than 40% of the sequences are shaded. Three parts of the Klarsicht-like domain are marked. (E) Alignment of 22 selected spectrin repeats of human NUANCE. The multiple alignment was made using the CLUSTAL W program (EMBL). The bars indicate positions of three helices according to the structure-based alignment of Winder and colleagues (Winder et al., 1995).

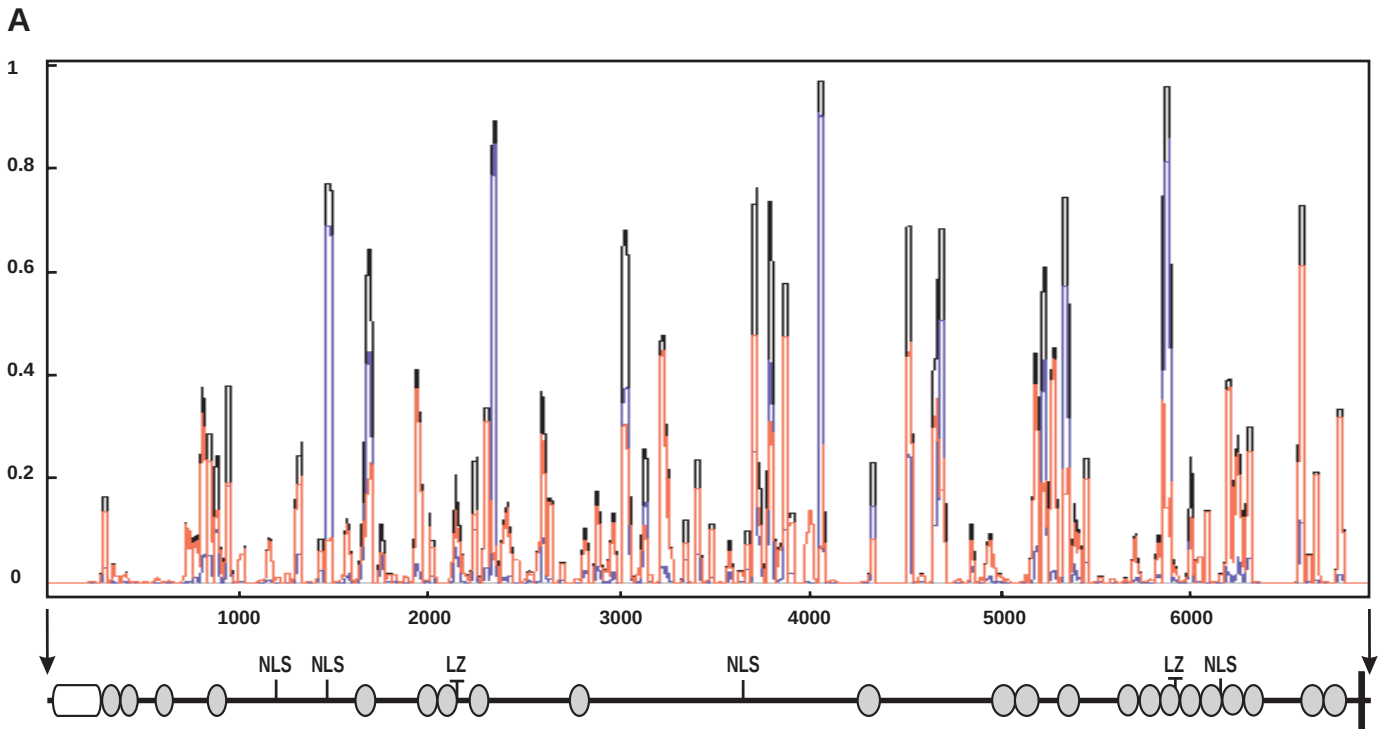
A
1
0.8
0.6
0.4
0.2
0
1000
2000
3000
4000
5000
6000
NLS
NLS
LZ
NLS
LZ
NLS

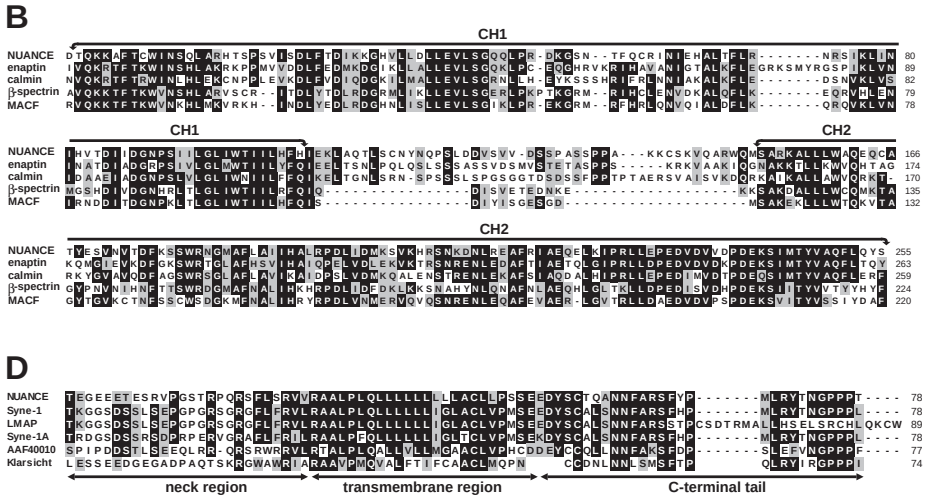
B
CH1
CH1
CH2
CH2
NUANCE
enaptin
calmin
β-spectrin
MACF

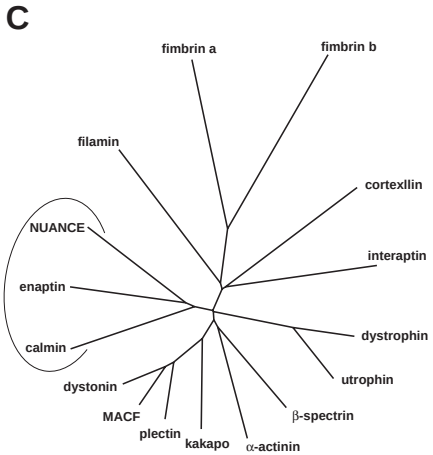
C
fimbrin a
fimbrin b
filamin
cortexllin
NUANCE
interaptin
enaptin
dystrophin
calmin
utrophin
dystonin
MACF
β-spectrin
plectin
kakapo
α-actinin

D
NUANCE
Syne-1
LMAP
Syne-1A
AAF40010
Klarsicht
neck region
transmembrane region
C-terminal tail

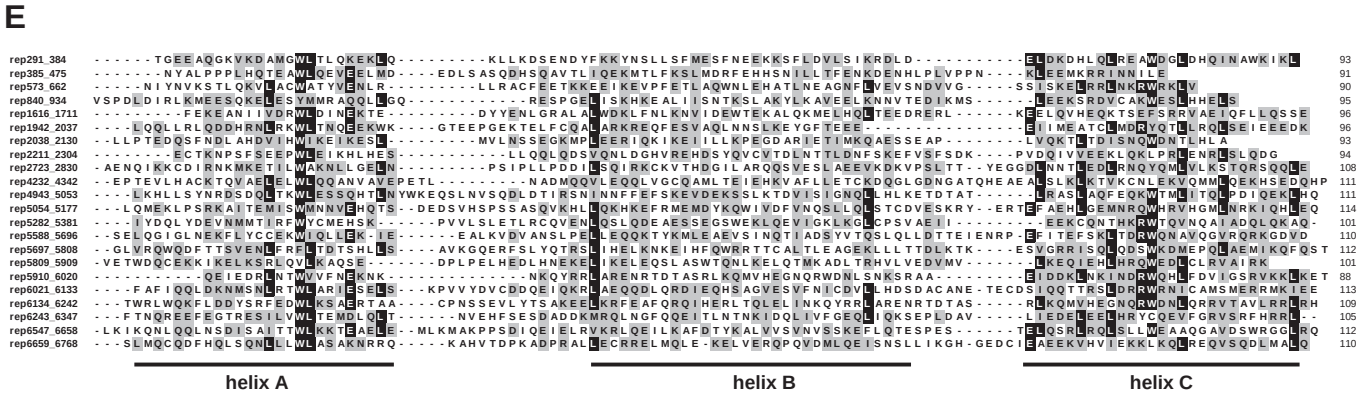
E
helix A
helix B
helix C

Fig. 3.

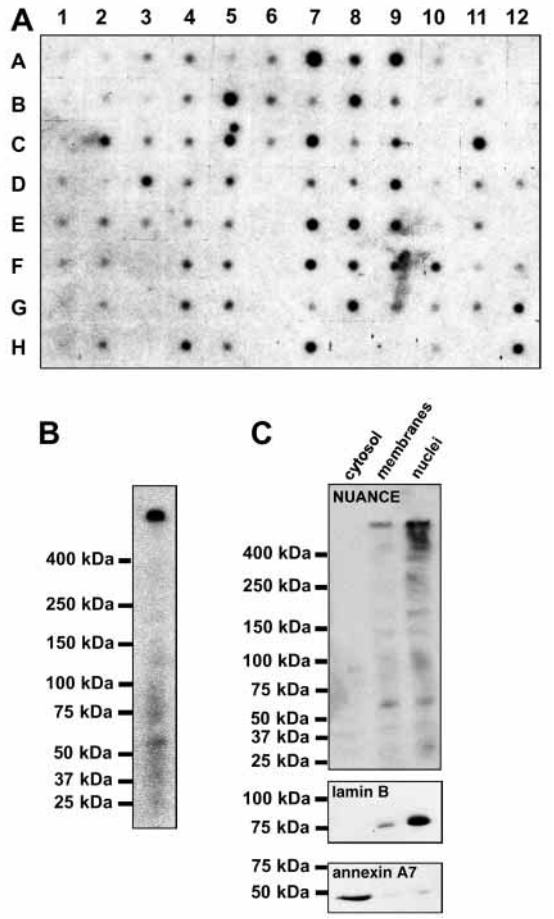

Fig. 4. Expression analysis of NUANCE. (A) A northern dot-blot of a variety of human tissues and cell lines, probed with a fragment corresponding to the ABD of NUANCE. These results are summarized in Table 2. Lane 12 represents controls: A12, yeast total RNA; B12, yeast tRNA; C12, *E. coli* rRNA; D12, *E. coli* DNA; E12, poly(A); F12 human C_0t_1 DNA; G12, human DNA 100 ng; H12, human DNA 500 ng. (B) Immunoblots of the COS7 cells homogenate. (C) Cells fractionated into nuclei, cytosol and cytoplasmic membranes. Each fraction was separated on 3-15% gradient SDS-PAGE and immunoblotted with anti-NUANCE, anti-lamin B and anti-annexin A7 mAbs as indicated. The positions of molecular mass marker proteins are shown on the left.

1999). The highly conserved hydrophobic stretch of 22 amino acids (residues 6848 to 6872) in the Klarsicht-like domain was identified as a transmembrane region (Fig. 3D). It is flanked by the N-terminally positioned neck region and the C-terminal tail.

Tissue distribution of NUANCE mRNA

In a Human Tissue Multiple Expression array containing mRNA from a variety of human tissues and cell lines we found that most of the tissues showed detectable levels of NUANCE mRNA. The highest expression was detected in the kidney, both adult and fetal, liver, stomach and placenta, and the lowest levels were in skeletal muscle and brain (Fig. 4A, Table 2). The corpus callosum and pituitary gland displayed a relatively strong signal in contrast to the generally low levels of expression in other parts of the brain. Expression of NUANCE

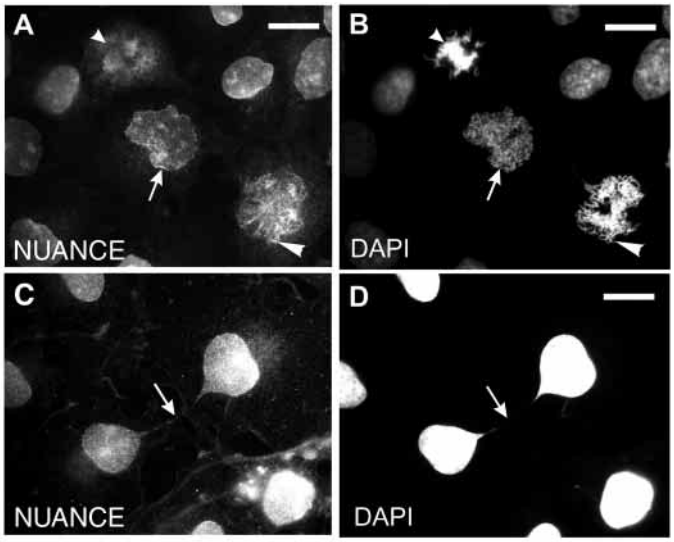

Fig. 5. Nuclear localization of NUANCE in COS7 cells (C,G) immunolabeled with the anti-NUANCE mAb K20-478. NUANCE remains associated with NE during prophase (A,B, arrow) and with chromosomes during prometaphase (A,B, large arrowhead). At later stages NUANCE is diffusely distributed throughout the cytoplasm (A, B, small arrowhead). NUANCE is also detected in bridges, which were occasionally seen between the nuclei of two cells (C,D, arrow). DNA was visualized with DAPI (B,D). Bar, 20 μm.

in lymphatic organs was not uniform either. High levels of mRNA were detected in spleen and lymphatic nodes; however they were relatively low in the thymus and hardly detectable in bone marrow. Taken together with the strong signal seen in peripheral blood lymphocytes, this suggests that NUANCE is characteristic for mature lymphocytes. In the digestive system only stomach, duodenum and salivary gland showed an elevated level of NUANCE mRNA relative to the other parts of the gastrointestinal tract. In addition, significant amounts of mRNA were also noted in the trachea, prostate, gonads, thyroid and adrenal glands. In RNA from cancer-derived cell lines, NUANCE was expressed at hardly traceable amounts with the exception of Daudi Burkitt's lymphoma cells.

NUANCE associates with nuclei

mAb K20-478 generated against the ABD of NUANCE recognized a protein of about 800 kDa that cofractionated with nuclei and membranes of COS7 cells (Fig. 4B,C). The mAbs against lamin B2 as nuclear protein and annexin A7 as mainly cytosolic protein were included as a control. Weaker bands below may represent degradation products of NUANCE, although they could also be short isoforms or crossreactive proteins. For size estimation, we included the A chain of EHS-laminin with a molecular mass of about 400,000, which migrated significantly faster than NUANCE (data not shown).

In immunofluorescence studies the mAb yielded a spotted rim-enriched nuclear labeling in Burkitt's lymphoma cells BL-60, human embryonic kidney cells 293 and COS7 cells (Fig. 5). In addition, a dotted pattern was detected in the cytoplasm, which might result from association with vesicular structures or ER (Fig. 5A,C). A similar pattern was observed in C3H/10T1/2 mouse fibroblasts (data not shown). NUANCE is also seen

Table 2. Expression of NUANCE in 76 human tissues

Tissue type	Expression level	Position on the grid*
Neurological		
Whole brain	tr	1A
Cerebral cortex	tr	1B
Frontal lobe	tr	1C
Parietal lobe	+	1D
Occipital lobe	+	1E
Temporal lobe	+	1F
Paracentral gyrus of cerebral cortex	tr	1G
Pons	tr	1H
Cerebellum, left	tr	2A
Cerebellum, right	tr	2B
Corpus callosum	++	2C
Amygdala	tr	2D
Caudate nucleus	+	2E
Hippocampus	+	2F
Medulla oblongata	+	2G
Putamen	+	2H
Substantia nigra	+	3A
Nucleus accumbens	tr	3B
Thalamus	+	3C
Pituitary gland	+++	3D
Spinal cord	+	3E
Muscle and heart		
Aorta	+	4B
Heart	+	4A
Atrium, left	+	4C
Atrium, right	+	4D
Ventricle, left	+	4E
Ventricle, right	++	4F
Interventricular septum	++	4G
Apex of the heart	++	4H
Skeletal muscle	+	7B
Gastro-intestinal		
Esophagus	tr	5A
Stomach	++++	5B
Duodenum	+++	5C
Jejunum	++	5D
Ileum	+	5E
Ileocecum	++	5F
Appendix	++	5G
Colon, ascending	+	5H
Colon, transverse	+	6A
Colon, descending	+	6B
Rectum	+	6C
Liver	++++	9A
Pancreas	+	9B
Salivary gland	+++	9E
Genito-urinary		
kidney	+++++	7A
bladder	+	8C
uterus	+	8D
prostate	++++	8E
testis	+++	8F
ovary	+++	8G
Lymphoid and hematopoetic		
Spleen	++++	7C
Thymus	+	7D
Lymph node	+++	7F
Bone morrow	+	7G
Peripheral blood leukocyte	++++	7E
Pulmonary		
Trachea	+++	7H
Lung	++	8A
Other		
Adrenal gland	++	9C
Thyroid gland	++++	9D
Mammary gland	++	9F
Cell lines		
Leukemia, HL-60	tr	10A
HeLa S3	tr	10B
Leukemia, K-562	tr	10C
Leukemia, MOLT-4	tr	10D
Burkitt´s lymphoma, Raji	tr	10E
Burkitt´s lymphoma, Daudi	++	10F
Colorectal adenocarcinoma, SW480	+	10G
Lung carcinoma, A549	tr	10H
Fetal and placenta		
Placenta	++++	8B
Fetal brain	tr	11A
Fetal heart	+	11B
Fetal kidney	++++	11C
Fetal liver	+	11D
Fetal spleen	+	11E
Fetal thymus	+	11F
Fetal lung	+	11G

*Grid references to Fig. 3A.
tr, traceable amounts.

associated with bridges that occasionally connected nuclei in COS7 cells (Fig. 5C,D). The punctate NUANCE staining of the nuclear surface was reminiscent of that of nucleoporins. A comparison of NUANCE and Nup358 distribution (Wu et al., 1995) however showed that both proteins are only partly colocalized (Fig. 6A-C), which implies that NUANCE is targeted to the NE without being localized to nuclear pores.

To clarify whether NUANCE is associated with the inner (INM) or outer nuclear membrane (ONM) we compared the immunostaining of the digitonin- and Triton X-100-permeabilized cells. Digitonin disrupts the plasmalemma leaving the intracellular membranes, including the NE, intact (Adam et al., 1990). As a result, the mAb can access ONM-associated antigens but not the proteins facing the nucleoplasm. The anti-NUANCE mAb stained only the nuclear periphery of the digitonin-permeabilized cells, which was similar to the staining for cytoplasm-facing nucleoporin 358 (Fig. 6J-L). The anti-lamin B2 mAb taken for a control did not yield any staining in digitonin-treated cells in interphasel; instead it labeled mitotic cells on the same cover slip (data not shown). This suggests that NUANCE associates with the ONM with its N-terminus facing the cytoplasm. However, it does not exclude its further association with the inner membrane of the envelope. In the Triton X-100-treated cells we also observed a labeling in the nucleus (Fig. 6D-I). It was especially enriched at nucleoli, which were identified using antiserum against the nucleolus protein NO38/B23 (G-I). Furthermore we always observed a diffuse cytoplasmic NUANCE staining that accumulated at the nuclear invagination harboring the Golgi apparatus (Fig. 6J), as

visualized with a β-COP-specific mAb (data not shown).

In mitotic cells NUANCE remains associated with the NE during its breakdown, which marks the end of prophase and beginning of prometaphase (Fig. 5A,B, arrows). This indicates a stable association of NUANCE with the NE. In prometaphase, NUANCE is accumulated at condensed chromosomes (Fig. 5A,B, large arrowheads) and is diffusely present throughout the cytoplasm at later stages (Fig. 5A, small arrowhead).

Sensitivity to agents affecting the cytoskeleton

The distribution pattern of NUANCE did not overlap with that of the actin cytoskeleton in spite of the presence of the predicted conserved ABD (Fig. 7A-C). To test whether disruption of the actin cytoskeleton affects NUANCE localization, we have treated COS7 cells with Latrunculin A (LatA), a drug depolymerizing actin filaments owing to its G-actin-sequestering activity (Yarmola et al., 2000). Already after 15 minutes exposure to 1 μM LatA, the actin filament meshwork was partially disassembled, and actin-rich foci were formed (data not shown). By 30 minutes, actin accumulated in the central area of the cell in which the NUANCE-positive 'cloud' was often seen at the invagination of the nuclei (Fig. 7D-F). Along with further disassembly of the actin cytoskeleton, the nuclei became less flattened and acquired an irregular shape with wrinkled invaginations from the side where a diffuse cytoplasmic pool of NUANCE and actin aggregates accumulated (Fig. 7G-I). This effect on nuclei was fully reversible. After 3 hours washout of LatA their shape was completely restored (not shown). This observation implies that the nuclear shape is controlled by the actin cytoskeleton and that NUANCE may have a structural role in maintaining the nuclear architecture.

In wound-healing assays performed on confluent monolayers of COS7 cells, NUANCE was detected at the leading edge of migrating cells colocalized with F-actin (Fig. 7J-L); this indicates partial redistribution of NUANCE in polarized cells.

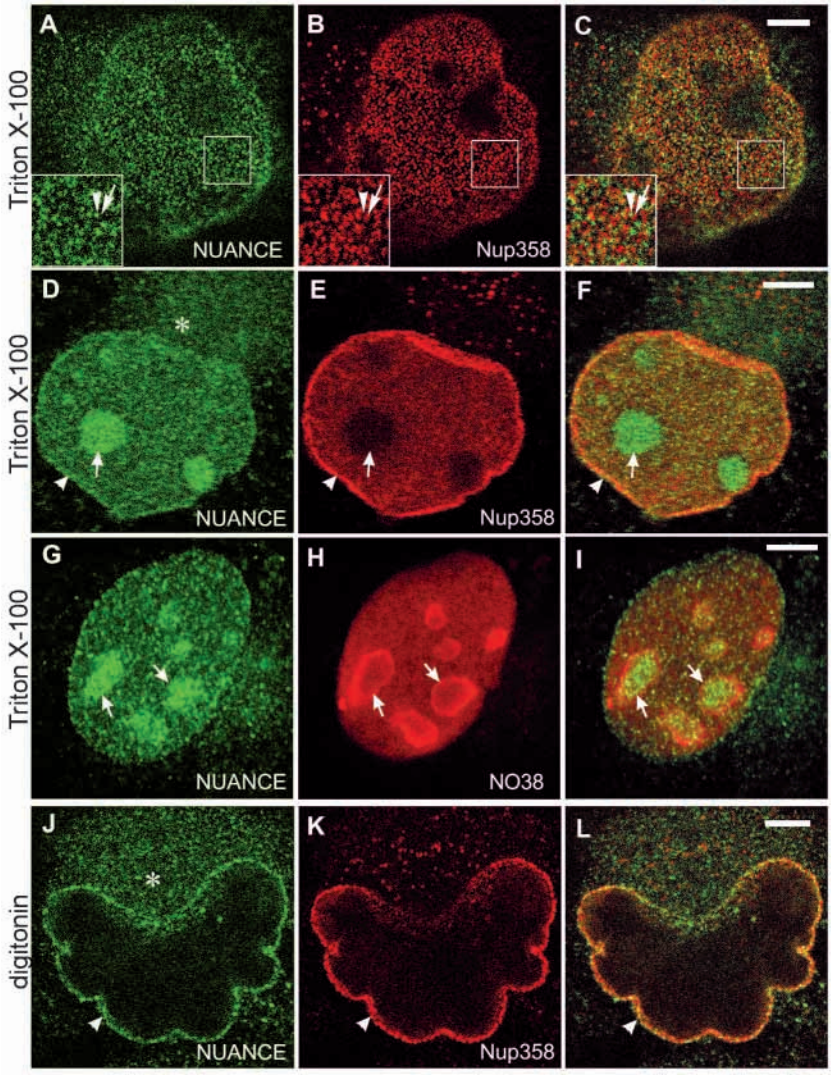

Fig. 6. Localization of NUANCE compared with that of nuclear pores. Cells were double labelled with anti-NUANCE (A,D,G,J) and anti-nucleoporin358 (Nup385) (B,E,K) antibodies. A-C, confocal sections of the apical part of a COS7 cell nucleus. The optical surfaces of nuclei are shown with enlargements of the regions indicated. NUANCE- (arrowheads, A-C) and Nup358-positive spots (arrows, A-C) are only partially colocalized. (D-L) The equatorial optical sections from the nuclei of COS7 cells, treated with 0.5% Triton X-100 (D-I) and 4 μM digitonin (J-L). Visualization of NUANCE at the NE in digitonin-treated cells (J-L, arrowheads) suggests its localization on the cytoplasmic face of the ONM. Note the polar distribution of cytoplasmic NUANCE (D, J, asterisk) and Nup385. In Triton X-100-treated cells, the intranuclear labeling was enriched in the nucleoli (D-I, arrows), which was verified by anti-NO38 staining (H). Bar, 5 μm.

We have also examined the pattern of NUANCE distribution upon treatment with vincristine and colchicine, drugs that disrupt selectively microtubules in the cell. However, no changes in nuclear morphology or in NUANCE distribution were observed (data not shown).

Domain analysis

The N-terminal actin-binding domain binds to F-actin in vitro and in vivo

As our immunofluorescence analysis revealed that association of NUANCE with the actin cytoskeleton is limited to the leading edge in migrating cells and to the perinuclear patches in LatA-treated cells, we examined the functionality and the subcellular localization of the ABD. For biochemical characterization of NUANCE we have used the recombinantly expressed ABD-containing construct 6×His-ABD. The 6×His-ABD associates with F-actin filaments in a high-speed cosedimentation assay (Fig. 8A). Some 6×His-ABD protein was present in the pellet without added actin; however it was always enriched in the pellets in the presence of actin-containing samples. The assay was performed with different

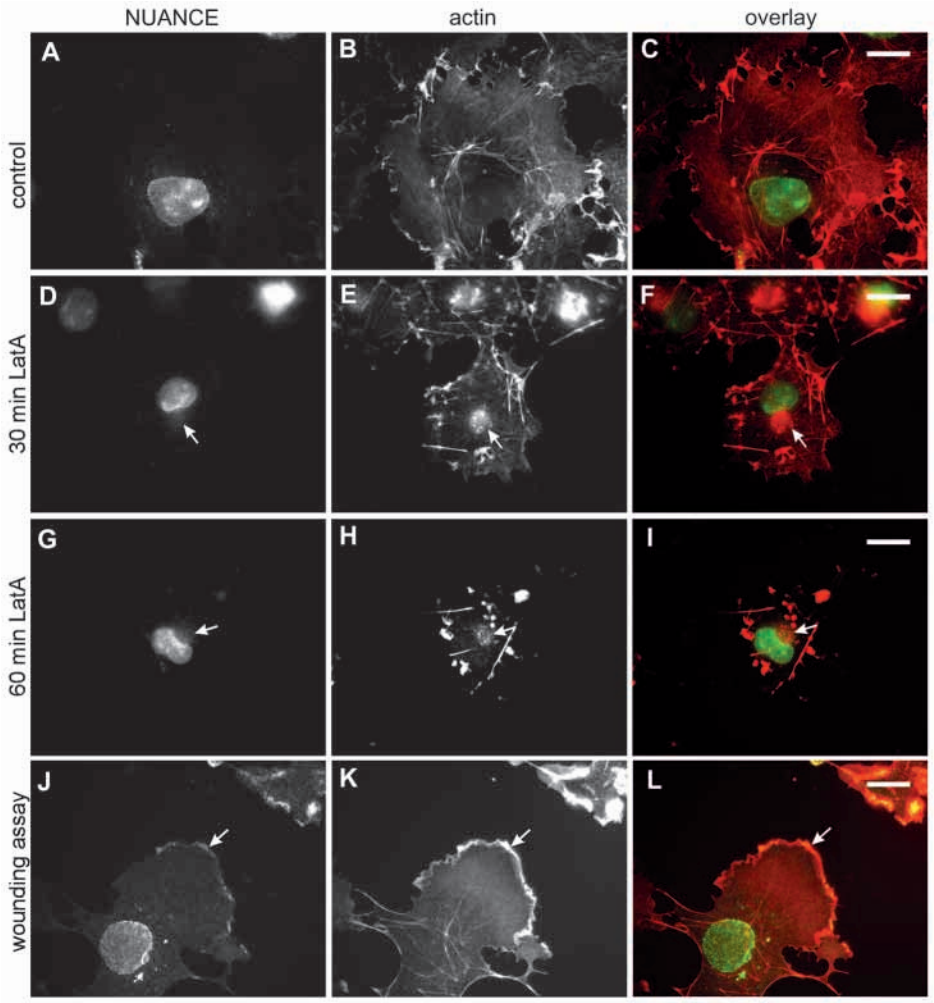

Fig. 7. Effect of LatA treatment on the subcellular distribution of endogenous NUANCE. COS7 cells were incubated in the absence (A-C) and presence (D-I) of 1 μM LatA for 30 minutes (D-F) and 60 minutes (G-I). (J-L) COS7 cells were stimulated to migrate by wounding a confluent monolayer of cells. 6 hours after wounding, the cells were processed for immunofluorescence microscopy. Cells were stained with an anti-NUANCE mAb followed by an Alexa-488-conjugated secondary antibody (A,D,G,J) and TRITC-phalloidin (B,E,H,K) to visualize actin filaments. (C-L) overlays. Bars, 20 μM.

concentrations of 6×His-ABD in order to quantify binding to F-actin. The K_d value was determined to be 3.8±1 μM, and saturation was achieved at a 1:1 molar ratio. The presence of 6×His-ABD also had an effect on the polymerization kinetics of pyrene-labeled actin (Fig. 8C). It shortened the elongation time and increased the rate of actin polymerization in a concentration-dependent manner. Moreover, in low-speed F-actin co-sedimentation assays most of the actin was detected in the pellet fraction, suggesting that NUANCE ABD acts to bundle F-actin (Fig. 8B).

We expressed GFP-fused ABD in COS7 cells and examined its subcellular distribution in vivo. In contrast to the endogenous protein, the GFP-ABD containing the 285 N-terminal amino acids of NUANCE was associated with all microfilament structures detectable by TRITC-phalloidin, stress fibers, lamellar meshwork and cortical actin (Fig. 9A,D). The GFP-ABD-S fusion protein, which corresponds to a short alternatively spliced isoform where insertion of an exon 8a introduced a stop codon in the second CH domain, showed a slightly different pattern. The GFP-ABD-S weakly associated with the middle parts of stress fibers but was enriched at their ends, which colocalized with the vinculin-labeled focal adhesions (Fig. 9B,E). Interestingly, the small focal complexes at the extreme edge of lamellipodia, which were not associated with stress fibers yet (Nobes and Hall, 1995), did not recruit the GFP-ABD-S (Fig. 9B,E). The GFP-ABD-S association with cortical actin was mainly confined to the bundles in retracting concave parts but not to the protruding lamellas. We also noted the formation of multiple spikes and filopodia in the cells strongly overexpressing GFP-ABD or GFP-ABD-S (data not shown). The filopodia-rich phenotype was presumably caused by the increased formation of actin bundles, which is in agreement with our in vitro observations. These proteins might therefore exhibit a dominant-negative effect. Moderate GFP-ABD expression did not seem to affect the organization of the actin cytoskeleton in COS7 cells.

Spectrin repeats1-2 and 15-21 of NUANCE seem to mediate membrane targeting

To explore the role of the spectrin repeats in actin association, we constructed a fusion protein GFP-ABDsr1-2 harboring a 531 amino acid fragment containing the ABD and the first two repeats (Fig. 9C,F). Costaining the GFP-ABDsr1-2-expressing cells with TRITC-phalloidin showed overall colocalization of the fusion protein with filamentous actin (data not shown). However, the GFP-ABDsr1-2 was strongly attracted to the subplasmalemmal regions, especially in protruding lamellas (Fig. 9C,F). This implies a role for the two spectrin repeats in membrane binding. The targeting of the stress fibers and focal contacts was reduced in comparison with the GFP-ABD and GFP-ABD-S proteins. The anti-NUANCE mAb recognized the GFP-ABDsr1-2 protein (Fig. 9F) as well as the other two ABD-containing chimeras (data not shown) and showed an identical pattern.

GFP-sr15-21 harboring spectrin repeats from 15 to 20 followed by the random coil stretch and a part of repeat 21 were used for the examination of the further spectrin repeats. The distribution pattern of the GFP-sr15-21 suggests its association with the intracellular membranes and with vesicular structures colocalizing with β-COP, a component of the COP coat (Fig. 9G,J). No association with the NE was detected.

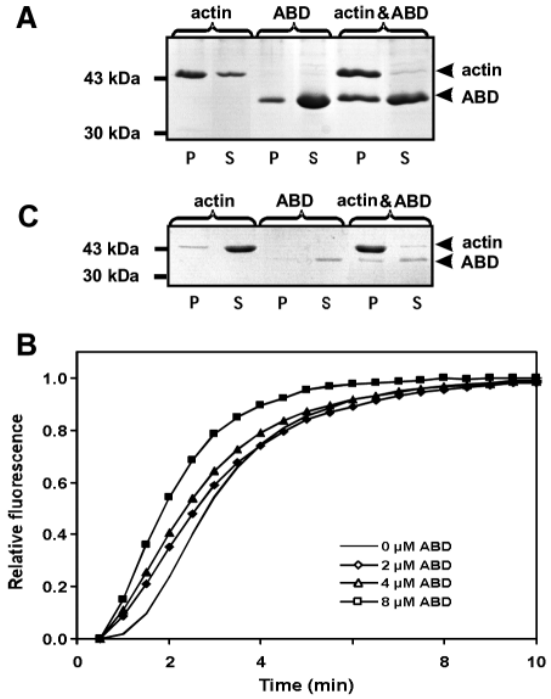

Fig. 8. Binding of 6×His-ABD to actin in vitro. (A) Cosedimentation of 10 μM 6×His-ABD with 2.5 μM F-actin by ultracentrifugation. (B) Bundling of 10 μM actin in the presence of 6×His-ABD analyzed by low-speed centrifugation. S, supernatant; P, pellet. Positions of ABD and actin are indicated on the right. (C) The effect on polymerization kinetics of 8 μM actin in the absence or presence of various amounts of 6×His-ABD observed by the change in pyrenyl-actin fluorescence.

The C-terminal transmembrane domain associates with the nuclear envelope

The NUANCE staining pattern appeared to be similar to the subcellular distribution of Syne-1, a protein that is associated with the NE in skeletal, cardiac and smooth muscle cells (Apel et al., 2000). As Syne-1 is highly homologous to the C-terminal part of NUANCE, the targeting of NUANCE to the NE could result from the Klarsicht-like domain at the C-terminus. To test our assumption we have prepared two C-terminal constructs, GFP-Cterm1 and GFP-Cterm2, comprising the Klarsicht-like domain and the preceding spectrin repeats. The GFP-Cterm1 protein possesses spectrin repeats 21 and 22, whereas the GFP-Cterm2 harbors only one complete repeat 22 but contains the additional 14 amino acids gained from the alternatively spliced exon 111. Both fusion proteins showed clear nuclear rim staining along with diffuse cytoplasmic staining in the Golgi area (Fig. 9H, shown for GFP-Cterm1). Moreover, both constructs seemed to displace endogenous NUANCE from the NE but did not interfere with the nucleoplasmic staining (Fig. 9K). In heavily overexpressing cells both GFP-Cterm1 and GFP-Cterm2 localized in patches at the NE and also showed a reticular or vesicular pattern in the cytoplasm (data not shown). To inspect whether the overexpression of the GFP-Cterm1 affects the nuclear pore distribution, we stained the transfected cells with the anti-Nup358 antibody. Confocal analysis reveals a mutually exclusive pattern of GFP patches and anti-Nup358 staining (Fig. 10A-C), suggesting the displacement of nuclear pores from the regions of GFP-Cterm1 accumulation. The appearance of lamins A/C and B, detected by the mAbs JOL2 and LN43, in contrast, was not affected in GFP-Cterm1- and GFP-Cterm2-expressing cells (data not shown). The overexpression of the C-terminal constructs did not hamper mitotic progression in COS7 cells. GFP-Cterm2, like the endogenous protein, remained associated with the NE during prophase, whereas the anti-Nup358 staining was largely diffuse (Fig. 10D-F), indicating at least partial disassembly of nuclear pores.

Fig. 9. Localization of GFP-fused chimeric proteins in transfected COS7 cells. Protein domains are presented as in Fig. 3. All GFP fusion protein comprising ABDs (A-F) were colocalized with actin stress fibers (A,C,D,F, big arrows) and actin meshwork throughout the cell as well as with the cortical actin in lamellae (C,F, arrowheads). The GFP-ABD-S was enriched at the tips of stress fibers (B,arrow) and diminished at the plasmalemma (B), whereas the GFP-ABDsr1-2 (C) associated stronger with the submembrane actin. Nascent focal complexes did not attract GFP-ABD-S (small arrowheads). The amino acids AYKN at the C-terminus of the GFP-ABD-S protein were encoded by the additional exon 8a found by PCR analysis. GFP-ABDsr1-2 protein (C,F) harbors two spectrin repeats in addition to the ABD. GFP-sr15-21, corresponding to the middle part of NUANCE from spectrin repeat 15 to 20, seems to target intracellular membranes and vesicular structures colocalizing with β-COP-positive structures (G,J, arrow) but not to the NE. By contrast, the GFP-Cterm1 protein harboring the TMD together with the two preceding spectrin repeats is recruited to the NE and adjacent ER (H). Note the lack of nuclear rim staining in the transfected cell (K, arrowhead). The GFP-Cterm2Δtm fusion protein is associated with vesicles but not with the NE (I,L, arrowheads). Cells transfected with the GFP-Cterm2Δtm construct were fixed with methanol (see details in the text). The transfected COS7 cells were double-labeled with TRITC-phalloidin (D), vinculin (E) and NUANCE (F,K,L) and β-COP (J) mAbs. Bar, 20 μm.

GFP-Cterm2Δtm, which is identical to GFP-Cterm2, but lacks the hydrophobic membrane-spanning sequence and the C-terminal tail, confirmed the importance of the TMD for the nuclear association. This protein was found in all cellular compartments when overexpressed in COS7 cells. However, in cells fixed with methanol, only vesicular staining in the cytoplasm remained (Fig. 9I). No nuclear staining was detected, and the localization of the endogenous NUANCE was not affected by the overexpression of the GFP-Cterm2Δtm (Fig. 9L). Thus, the TMD is necessary for recruitment to the NE. These results suggest that NUANCE is an integral protein of the NE that shares the TMD with the other proteins exhibiting a similar subcellular localization.

Having identified the intracellular locations for N-terminal and C-terminal parts of NUANCE we generated a construct GFP-NUA$^{\Delta 460\text{-}6643}$ where the first 459 amino acids were directly fused to the C-terminal 315 amino acids that correspond to the Cterm1 construct. In transfected COS7 cells, the GFP-NUA$^{\Delta 460\text{-}6643}$ was arranged in various structures from fine filaments to large aggregates (Fig. 10G-L). In most of the cells, the GFP-NUA$^{\Delta 460\text{-}6643}$ was observed at the NE envelope, enriched at one side of the nucleus (Fig. 10J-L). Actin was often attracted to the GFP-NUA$^{\Delta 460\text{-}6643}$ fibers and aggregates; however, GFP-NUA$^{\Delta 460\text{-}6643}$ was never seen in association with the dynamic submembranous actin cytoskeleton.

Discussion

NUANCE, a transmembrane protein associated with actin and the nuclear envelope

Cloning of the NUANCE cDNA yielded the largest protein of

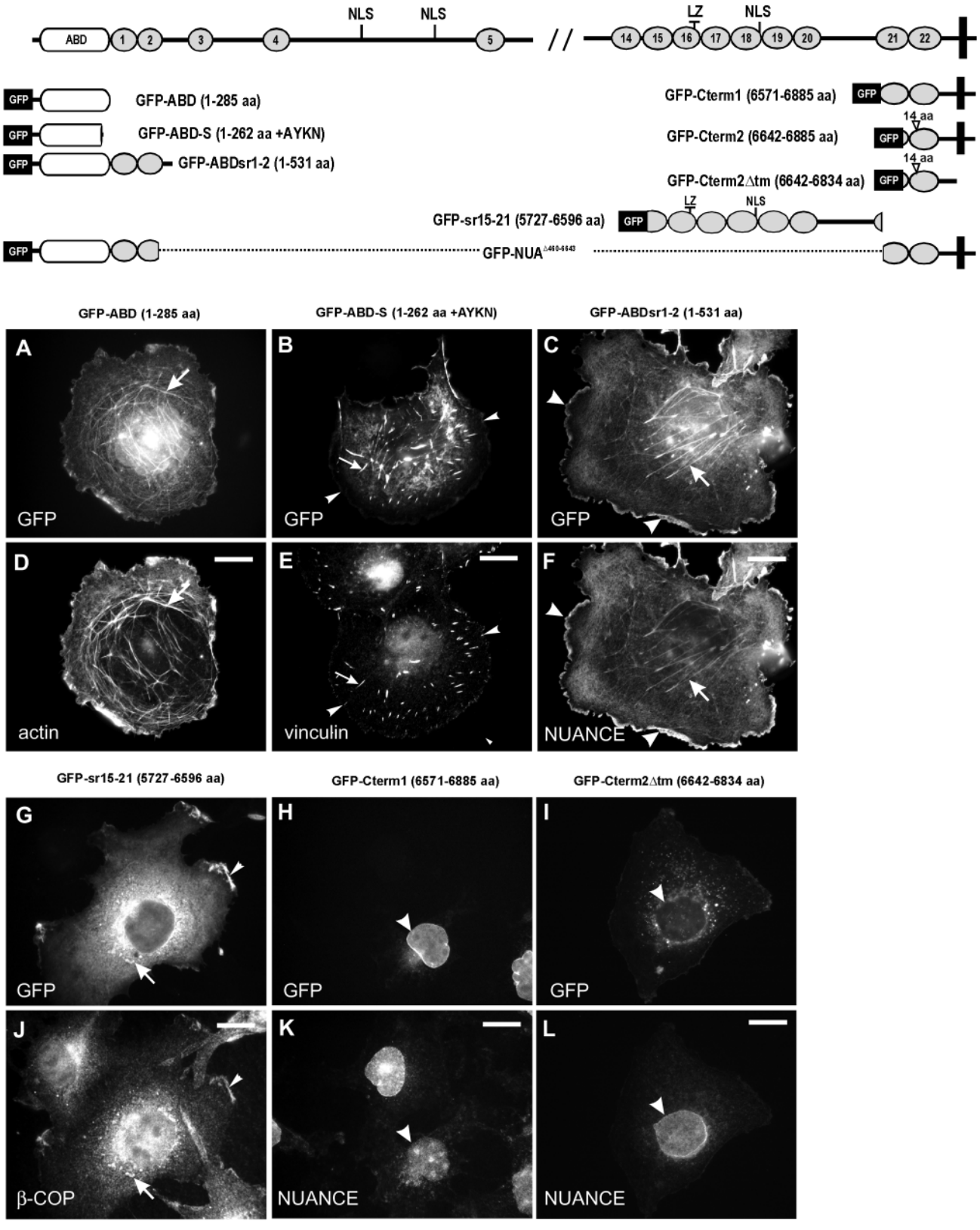

the α-actinin superfamily that has so far been characterized. It is conceivable that NUANCE forms dimers or even higher order oligomers since it has an extremely long largely coiled-coil rod with two leucine-zippers. NUANCE is localized at the NE, which is rather unusual for actin-binding proteins. The NUANCE ABD appears to bind to F-actin in vitro and in vivo and promote actin bundling. Moreover, transfection with the GFP-NUA$^{\Delta 460\text{-}6643}$ mutant has resulted in significant

recruitment of F-actin to the nuclear membrane. This difference between the NUA$^{\Delta 460\text{-}6643}$ and wild-type phenotypes indicates that the ABD of the full-length NUANCE could be regulated in vivo, for instance by adopting a conformation with the actin-binding sites being hidden. Two other proteins, calmin and *Dictyostelium* interaptin, which likewise possess ABDs at the N-termini and TMDs at the C-termini, associate with cytoplasmic reticular structures and, in the case of interaptin, with the NE (Rivero et al. 1998; Ishisaki et al., 2001). The predicted TMDs of these three proteins show very low homology and may be responsible for the differential intracellular localization.

NUANCE appears to be recruited to the NE through the Klarsicht-like C-terminal domain harboring a TMD. *Drosophila* Klarsicht protein is required for migration of nuclei in developing retinal photoreceptors (Mosley-Bishop et al., 1999). Similarly, a role in the migration of micronuclei in myotubes and/or their anchoring at the postsynaptic apparatus was ascribed to Syne-1 (Apel et al., 2000), a protein that is highly homologous to the C-terminal part of NUANCE. Syne-1 is selectively associated with the nuclei that lie beneath the postsynaptic membrane at the neuromuscular junctions in skeletal, cardiac and smooth muscle cells. Syne-1 is strongly expressed in the muscle and brain, tissues with the lowest level of NUANCE expression. Since the N-terminus of the longest Syne-1 isoform has not yet been identified, it is plausible that the full-length Syne-1 protein also possesses an N-terminal ABD and therefore may represent a muscle/brain counterpart of NUANCE. Nuclear positioning and migration are essential for the movement of pronuclei during fertilization, normal mitotic and meiotic cell division and various morphogenetic processes during metazoan development. Nuclear migration has been directly linked to a human disease, the brain developmental disorder lissencephaly (Morris, 2000). Migration of neurons involves nucleokinesis, a process whereby cells acquire an elongated shape or extend a frontal protrusion, and the nucleus migrates to its new position within the cytoplasm. The nuclear translocation within the cell can also be associated with cell motility during tumor cell invasion. In moving fibroblasts, the classical model for cell motility studies, the nucleus remains centrally anchored within the cell despite drastic morphological changes. However, the human lung adenocarcinoma cells, which generally display a fibroblast-like motility, can be switched to the characteristic pattern of cell translocation with nucleokinesis as a distinct

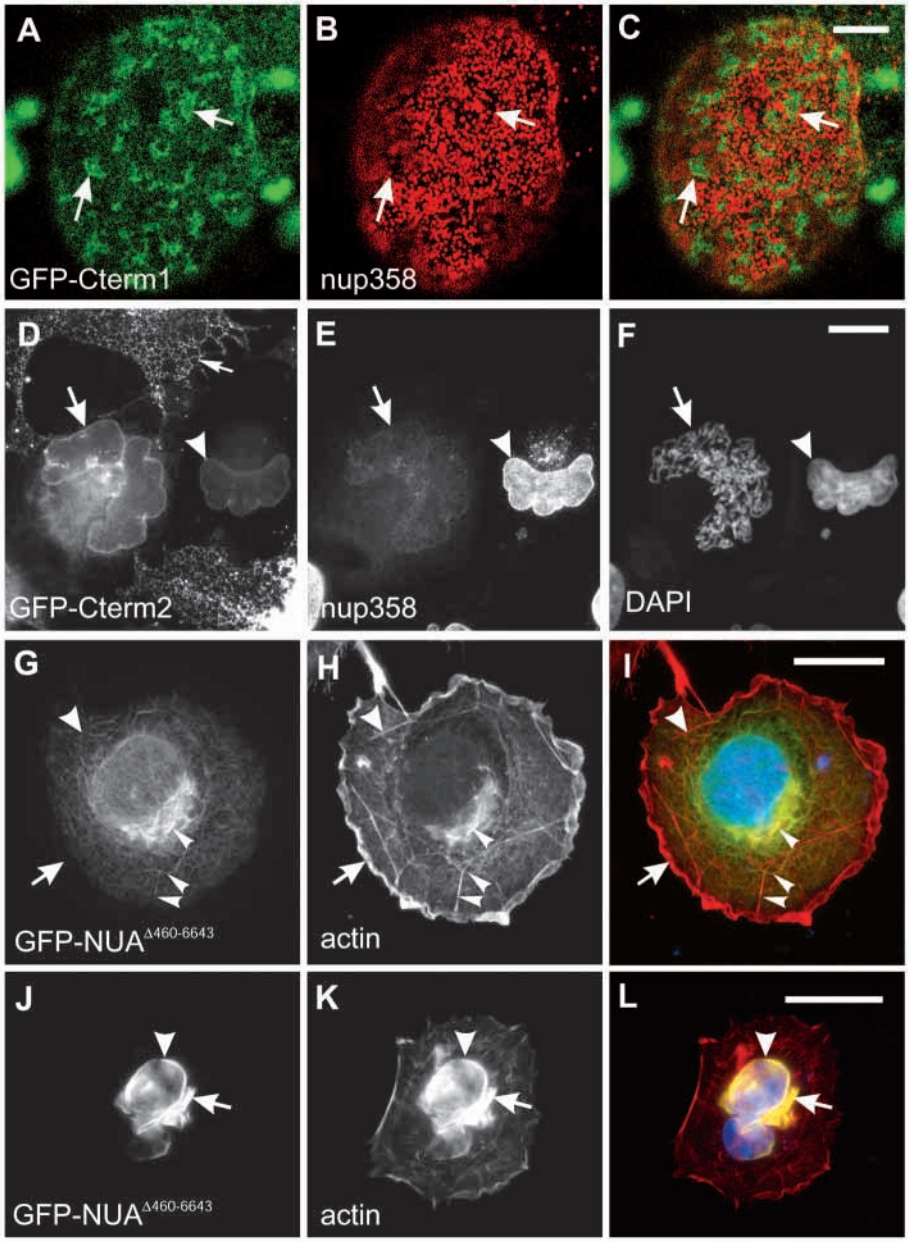

Fig. 10. The C-terminal domain of NUANCE targets the NE. (A-C) Confocal optical section through the apical part of the COS7 nucleus showing that the overexpressed GFP-Cterm1 protein was arranged in patches displacing nuclear pores (arrows), detected by anti-Nup358 antibody (B). (D-F) The GFP-Cterm2 remained associated with the NE in prophase (D, arrow) when the nuclear pores begin to disassemble as indicated by diffuse anti-Nup358 staining (E). DNA was visualized with DAPI (F,I,L). (J-L) Two examples of the cellular localization of the GFP-NUA$^{\Delta 460\text{-}6643}$ overexpressed in COS7 cells stained with TRITC-phalloidin (H,K). The GFP-NUA$^{\Delta 460\text{-}6643}$ possesses the N-terminal ABD and the C-terminal Klarsicht-like domain but lacks most of the central rod domain. The GFP-NUA$^{\Delta 460\text{-}6643}$ is arranged in fibers (G-I, small arrowheads) or perinuclear aggregates (J-L, arrows) partially colocalizing with actin. Dynamic cortical cytoskeleton (G-I, arrow) and some of the stress fibers (G-I, large arrowhead) do not recruit GFP-NUA$^{\Delta 460\text{-}6643}$. (I,L) show overlays of the GFP, TRITC and DAPI channels. Bars (A-C) 5 μM; (D-F) 10 μM; (J-L) 20 μM.

step in response to an autocrine motility factor (Klominek et al., 1991). The motility steps of the invasion process have been proposed to comprise protrusion of the tumor cell pseudopodia through surrounding tissues, followed by nucleokinesis and, finally, retraction of the pseudopodia behind the nucleus.

On the basis of the data accumulated on NUANCE, we can envision several roles for it. Rapid shrinkage of the nuclei accompanied by the accumulation of cytoplasmic NUANCE and actin at the side of the nucleus in the LatA-treated cells suggests that the actin cytoskeleton is implicated in controlling nuclear shape and that this process could be mediated by NUANCE. In addition to a role in nuclear positioning and/or migration, NUANCE may also contribute to the mechanical connection between cell surface receptors, cytoskeletal filaments and nuclear scaffolds. Such a coordinated response to mechanical stress was demonstrated by micromanipulation of integrins, which resulted in changes in nuclear shape that may influence gene expression (Chicurel et al., 1998). Maintenance of the nuclear shape and polarity could be essential for many cell types undergoing mechanical stress in vivo, as for instance, for lymphocytes when transgressing the blood vessels.

Eight integral proteins of the NE have so far been identified. Six of them are located at the INM. These are lamina-associated polypepetide (LAP)1 (Senior and Gerace, 1988), LAP2/thymopoietin (Foisner and Gerace, 1993), p58/lamin B receptor (LBR) (Worman et al., 1988), emerin (Nagano et al., 1996), nurim (Rolls et al., 1999) and MAN1 (Lin et al., 2000). Two integral proteins, POM121and gp210, have been found to be specific for the nuclear pore membrane (Gerace et al., 1982; Soderqvist and Hallberg, 1994). All of them are arranged with their N-termini facing the nucleoplasm. The discovery of NUANCE as the first example of a protein, which seems to associate specifically with the ONM, implies that the ONM represents a membrane subdomain that is biochemically and functionally distinct from the peripheral ER. Recent studies demonstrated that the dynein-dynactin complex is recruited to the cytoplasmic face of the NE during late G2 and early prophase prior to the NE breakdown and plays a role in tearing the NE at the beginning of mitosis (Beaudouin et al., 2002; Salina et al., 2002). Our data suggest that the N-terminal part of NUANCE faces the cytoplasm thereby allowing the protein to represent a platform for anchoring the dynein-dynactin complexes at the ONM. Interestingly, the NE wrinkles observed at the sites of invaginations of the ‘kidney bean’-shaped nuclei in the LatA-treated cells resemble the microtubules containing finger-like projections of the prophase and prometaphase cells. Furthermore, accumulation of F-actin and the cytoplasmic NUANCE at the sites of nuclear invaginations upon LatA treatment imply a link between NUANCE and pericentrosomal astral complex. Although at present we have no evidence of a functional relationship between NUANCE and NE breakdown, it is possible that NUANCE is involved in the spatial organization of microtubule-dependent machinery linking it to the NE.

Our results with digitonin-treated cells do not exclude an association of NUANCE with the INM where it might face the nucleoplasm with its ABD and interact with nuclear actin whose role is still elusive (Rando et al., 2000). NUANCE staining was also observed throughout the nucleoplasm and in nucleoli. These forms might well represent differentially spliced variants lacking the TMD. Such isoforms may build a fibrous meshwork in the nucleoplasm by oligomerizating via leucine zippers of the coiled coil. Although we have not identified TMD-lacking transcripts in our screen yet, their existence is quite plausible since many membrane proteins including calmin are differentially spliced and give rise to soluble isoforms (Ishisaki et al., 2001). It can be speculated that NUANCE plays a role in the organization of the intranuclear space. It was shown that actin is associated with the nucleoplasmic filaments of nuclear pore complexes and is involved in nuclear export (Hofmann et al., 2001). A role of NUANCE in nuclear export would explain its partial colocalization with nuclear pores. Actin may also be important for packaging the RNA into a Balbiani ring particles and their translocation through the nuclear pores to the cytoplasm (Percipalle et al., 2001). In a complex with actin, NUANCE may play a role in location and transportation of proteins and RNA within the nucleoplasm. The observation of NUANCE in nucleoli is particularly intriguing. The nucleoli are structures responsible mainly for ribosomal biogenesis; however they also participate in processing or export of some mRNAs and tRNAs (Schneiter et al., 1995; Bertrand et al., 1998) and are involved in sequestering cell cycle regulating proteins (Visintin and Amon, 2000). NUANCE would make an ideal candidate for organizing the nucleoli matrix and ensuring its compartmentalization and integrity.

This work was supported by a grant from the Center for Molecular Medicine Cologne and by a Köln Fortune studentship to T.L. We thank Elias Coutavas and Günter Blobel (The Rockefeller University, USA) for providing anti-Nup358 antibodies, Frans Ramaekers and Jos Broers (University of Maastricht, the Netherlands) for the gift of anti-lamin A/C and anti-lamin B1 antibodies, Marion Schmidt-Zachmann for the gift of anti-NO38/B23 antiserum, Mats Paulsson (University of Cologne) for laminin, Michael Schleicher (University of Munich, Germany) for sharing reagents and Prof. Diehl (University of Cologne, Germany) for providing the lymphoma cell lines.

References

Adam, S. A., Marr, R. S. and Gerace, L. (1990). Nuclear protein import in permeabilized mammalian cells requires soluble cytoplasmic factors. *J. Cell Biol.* **111**, 807-816.

Ahn, A. H. and Kunkel, L. M. (1993). The structural and functional diversity of dystrophin. *Nat. Genet.* **3**, 283-291.

Apel, E. D., Lewis, R. M., Grady, R. M. and Sanes, J. R. (2000). Syne-1, a dystrophin- and Klarsicht-related protein associated with synaptic nuclei at the neuromuscular junction. *J. Biol. Chem.* **275**, 31986-31995.

Beaudouin, J., Gerlich, D., Daigle, N., Eils, R. and Ellenberg, J. (2002). Nuclear envelope breakdown proceeds by microtubule-induced tearing of the lamina. *Cell* **108**, 83-96.

Bertrand, E., Houser-Scott, F., Kendall, A., Singer, R. H. and Engelke, D. R. (1998). Nucleolar localization of early tRNA processing. *Genes Dev.* **12**, 2463-2468.

Breathnach, R. and Chambon, P. (1981). Organization and expression of eucaryotic split genes coding for proteins. *Annu. Rev. Biochem.* **50**, 349-383.

Brown, A., Bernier, G., Mathieu, M., Rossant, J. and Kothary, R. (1995). The mouse dystonia musculorum gene is a neural isoform of bullous pemphigoid antigen 1. *Nat. Genet.* **10**, 301-306.

Chicurel, M. E., Singer, R. H., Meyer, C. J. and Ingber, D. E. (1998). Integrin binding and mechanical tension induce movement of mRNA and ribosomes to focal adhesions. *Nature* **392**, 730-733.

Foisner, R. and Gerace, L. (1993). Integral membrane proteins of the nuclear envelope interact with lamins and chromosomes, and binding is modulated by mitotic phosphorylation. *Cell* **73**, 1267-1279.

Fuchs, E. and Yang, Y. (1999). Crossroads on cytoskeletal highways. *Cell* **98**, 547-550.

Gerace, L., Ottaviano, Y. and Kondor-Koch, C. (1982). Identification of a major polypeptide of the nuclear pore complex. *J. Cell Biol.* **95**, 826-837.

Gregory, S. L. and Brown, N. H. (1998). kakapo, a gene required for adhesion between and within cell layers in *Drosophila*, encodes a large cytoskeletal linker protein related to plectin and dystrophin. *J. Cell Biol.* **143**, 1271-1282.

Hofmann, W., Reichart, B., Ewald, A., Muller, E., Schmitt, I., Stauber, R. H., Lottspeich, F., Jockusch, B. M., Scheer, U., Hauber, J. and Dabauvalle, M. C. (2001). Cofactor requirements for nuclear export of Rev response element (RRE)- and constitutive transport element (CTE)-containing retroviral RNAs. An unexpected role for actin. *J. Cell Biol.* **152**, 895-910.

Ishisaki, Z., Takaishi, M., Furuta, I. and Huh, N. (2001). Calmin, a protein with calponin homology and transmembrane domains expressed in maturing spermatogenic cells. *Genomics* **74**, 172-179.

Karakesisoglou, I., Yang, Y. and Fuchs, E. (2000). An epidermal plakin that integrates actin and microtubule networks at cellular junctions. *J. Cell Biol.* **149**, 195-208.

Klominek, J., Sundqvist, K. G. and Robert, K. H. (1991). Nucleokinesis: distinct pattern of cell translocation in response to an autocrine motility factor-like substance or fibronectin. *Proc. Natl. Acad. Sci. USA* **88**, 3902-3906.

Korenbaum, E., Nordberg, P., Bjorkegren-Sjogren, C., Schutt, C. E., Lindberg, U. and Karlsson, R. (1998). The role of profilin in actin polymerization and nucleotide exchange. *Biochemistry* **37**, 9274-9283.

Kozak, M. (1987). An analysis of 5′-noncoding sequences from 699 vertebrate messenger RNAs. *Nucleic Acids Res.* **15**, 8125-8148.

Laemmli, U. K. (1970). Cleavage of structural proteins during the assembly of the head of bacteriophage T4. *Nature* **227**, 680-685.

Leung, C. L., Sun, D., Zheng, M., Knowles, D. R. and Liem, R. K. (1999). Microtubule actin cross-linking factor (MACF): a hybrid of dystonin and dystrophin that can interact with the actin and microtubule cytoskeletons. *J. Cell Biol.* **147**, 1275-1286.

Leung, C. L., Liem, R. K., Parry, D. A. and Green, K. J. (2001a). The plakin family. *J. Cell Sci.* **114**, 3409-3410.

Leung, C. L., Zheng, M., Prater, S. M. and Liem, R. K. (2001b). The BPAG1 locus: Alternative splicing produces multiple isoforms with distinct cytoskeletal linker domains, including predominant isoforms in neurons and muscles. *J. Cell Biol.* **154**, 691-697.

Lin, F., Blake, D. L., Callebaut, I., Skerjanc, I. S., Holmer, L., McBurney, M. W., Paulin-Levasseur, M. and Worman, H. J. (2000). MAN1, an inner nuclear membrane protein that shares the LEM domain with lamina-associated polypeptide 2 and emerin. *J. Biol. Chem.* **275**, 4840-4847.

Matsudaira, P. (1994). Actin crosslinking proteins at the leading edge. *Semin. Cell Biol.* **5**, 165-174.

Morris, N. R. (2000). Nuclear migration. From fungi to the mammalian brain. *J. Cell Biol.* **148**, 1097-1101.

Mosley-Bishop, K. L., Li, Q., Patterson, L. and Fischer, J. A. (1999). Molecular analysis of the klarsicht gene and its role in nuclear migration within differentiating cells of the *Drosophila* eye. *Curr. Biol.* **9**, 1211-1220.

Nagano, A., Koga, R., Ogawa, M., Kurano, Y., Kawada, J., Okada, R., Hayashi, Y. K., Tsukahara, T. and Arahata, K. (1996). Emerin deficiency at the nuclear membrane in patients with Emery-Dreifuss muscular dystrophy. *Nat. Genet.* **12**, 254-259.

Nobes, C. D. and Hall, A. (1995). Rho, rac and cdc42 GTPases regulate the assembly of multimolecular focal complexes associated with actin stress fibres, lamellipodia and filopodia. *Cell* **81**, 53-62.

Okuda, T., Matsuda, S., Nakatsugawa, S., Ichigotani, Y., Iwahashi, N., Takahashi, M., Ishigaki, T. and Hamaguchi, M. (1999). Molecular cloning of macrophin, a human homologue of *Drosophila* kakapo with a close structural similarity to plectin and dystrophin. *Biochem. Biophys. Res. Commun.* **264**, 568-574.

Olski, T. M., Noegel, A. A. and Korenbaum, E. (2001). Parvin, a 42 kDa focal adhesion protein, related to the alpha-actinin superfamily. *J. Cell Sci.* **114**, 525-538.

Pascual, J., Castresana, J. and Saraste, M. (1997). Evolution of the spectrin repeat. *Bioessays* **19**, 811-817.

Pepperkok, R., Scheel, J., Horstmann, H., Hauri, H. P., Griffiths, G. and Kreis, T. E. (1993). Beta-COP is essential for biosynthetic membrane transport from the endoplasmic reticulum to the Golgi complex in vivo. *Cell* **74**, 71-82.

Percipalle, P., Zhao, J., Pope, B., Weeds, A., Lindberg, U. and Daneholt, B. (2001). Actin bound to the heterogeneous nuclear ribonucleoprotein hrp36 is associated with Balbiani ring mRNA from the gene to polysomes. *J. Cell Biol.* **153**, 229-236.

Prokop, A., Uhler, J., Roote, J. and Bate, M. (1998). The kakapo mutation affects terminal arborization and central dendritic sprouting of *Drosophila* motorneurons. *J. Cell Biol.* **143**, 1283-1294.

Puius, Y. A., Mahoney, N. M. and Almo, S. C. (1998). The modular structure of actin-regulatory proteins. *Curr. Opin. Cell Biol.* **10**, 23-34.

Rando, O. J., Zhao, K. and Crabtree, G. R. (2000). Searching for a function for nuclear actin. *Trends Cell Biol.* **10**, 92-97.

Rivero, F., Kuspa, A., Brokamp, R., Matzner, M. and Noegel, A. A. (1998). Interaptin, an actin-binding protein of the alpha-actinin superfamily in Dictyostelium discoideum, is developmentally and cAMP-regulated and associates with intracellular membane compartments. *J. Cell Biol.* **142**, 735-750.

Rolls, M. M., Stein, P. A., Taylor, S. S., Ha, E., McKeon, F. and Rapoport, T. A. (1999). A visual screen of a GFP-fusion library identifies a new type of nuclear envelope membrane protein. *J. Cell Biol.* **146**, 29-44.

Ruhrberg, C. and Watt, F. M. (1997). The plakin family: versatile organizers of cytoskeletal architecture. *Curr. Opin. Genet. Dev.* **7**, 392-397.

Salina, D., Bodoor, K., Eckley, D. M., Schroer, T. A., Rattner, J. B. and Burke, B. (2002). Cytoplasmic dynein as a facilitator of nuclear envelope breakdown. *Cell* **108**, 97-107.

Schneiter, R., Kadowaki, T. and Tartakoff, A. M. (1995). mRNA transport in yeast: time to reinvestigate the functions of the nucleolus. *Mol. Biol. Cell* **6**, 357-370.

Selbert, S., Fischer, P., Pongratz, D., Stewart, M. and Noegel, A. A. (1995). Expression and localization of annexin VII (synexin) in muscle cells. *J. Cell Sci.* **108**, 85-95.

Senior, A. and Gerace, L. (1988). Integral membrane proteins specific to the inner nuclear membrane and associated with the nuclear lamina. *J. Cell Biol.* **107**, 2029-2036.

Soderqvist, H. and Hallberg, E. (1994). The large C-terminal region of the integral pore membrane protein, POM121, is facing the nuclear pore complex. *Eur. J. Cell Biol.* **64**, 186-191.

Strumpf, D. and Volk, T. (1998). Kakapo, a novel cytoskeletal-associated protein is essential for the restricted localization of the neuregulin-like factor, vein, at the muscle-tendon junction site. *J. Cell Biol.* **143**, 1259-1270.

Sun, Y., Zhang, J., Kraeft, S. K., Auclair, D., Chang, M. S., Liu, Y., Sutherland, R., Salgia, R., Griffin, J. D., Ferland, L. H. et al. (1999). Molecular cloning and characterization of human trabeculin-alpha, a giant protein defining a new family of actin-binding proteins. *J. Biol. Chem.* **274**, 33522-33530.

Tinsley, J. M., Blake, D. J., Roche, A., Fairbrother, U., Riss, J., Byth, B. C., Knight, A. E., Kendrick-Jones, J., Suthers, G. K., Love, D. R. et al. (1992). Primary structure of dystrophin-related protein. *Nature* **360**, 591-593.

Visintin, R. and Amon, A. (2000). The nucleolus: the magician's hat for cell cycle tricks. *Curr. Opin. Cell Biol.* **12**, 372-377.

Wiche, G. (1998). Domain structure and transcript diversity of plectin. *Biol. Bull.* **194**, 381-383.

Wiche, G., Becker, B., Luber, K., Weitzer, G., Castanon, M. J., Hauptmann, R., Stratowa, C. and Stewart, M. (1991). Cloning and sequencing of rat plectin indicates a 466-kD polypeptide chain with a three-domain structure based on a central alpha-helical coiled coil. *J. Cell Biol.* **114**, 83-99.

Winder, S. J., Gibson, T. J. and Kendrick-Jones, J. (1995). Dystrophin and utrophin: the missing links! *FEBS Lett.* **369**, 27-33.

Wolf, E., Kim, P. S. and Berger, B. (1997). MultiCoil: a program for predicting two- and three-stranded coiled coils. *Protein Sci.* **6**, 1179-1189.

Worman, H. J., Yuan, J., Blobel, G. and Georgatos, S. D. (1988). A lamin B receptor in the nuclear envelope. *Proc. Natl. Acad. Sci. USA* **85**, 8531-8534.

Wu, J., Matunis, M. J., Kraemer, D., Blobel, G. and Coutavas, E. (1995). Nup358, a cytoplasmically exposed nucleoporin with peptide repeats, Ran-GTP binding sites, zinc fingers, a cyclophilin A homologous domain, and a leucine-rich region. *J. Biol. Chem.* **270**, 14209-14213.

Yarmola, E. G., Somasundaram, T., Boring, T. A., Spector, I. and Bubb, M. R. (2000). Actin-latrunculin A structure and function. Differential modulation of actin-binding protein function by latrunculin A. *J. Biol. Chem.* **275**, 28120-28127.